

Insights into the diet and feeding behavior of immature polar cod (*Boreogadus saida*) from the under-ice habitat of the central Arctic Ocean

Fokje L. Schaafsma¹  | Hauke Flores² | Carmen L. David^{3,4} | Giulia Castellani² | Serdar Sakinan¹ | André Meijboom¹ | Barbara Niehoff² | Astrid Cornils² | Nicole Hildebrandt² | Katrin Schmidt⁵ | Pauline Snoeijns-Leijonmalm⁶ | Julia Ehrlich^{2,7} | Carin J. Ashjian⁴ | the MOSAiC team ECO

¹Wageningen Marine Research, Den Helder, The Netherlands

²Department of Polar Biological Oceanography, Alfred Wegener Institute Helmholtz Center for Polar and Marine Research, Bremerhaven, Germany

³Marine Animal Ecology Group, Wageningen University, Wageningen, The Netherlands

⁴Department of Biology, Woods Hole Oceanographic Institution, Woods Hole, Massachusetts, USA

⁵School of Geography, Earth and Environmental Sciences, University of Plymouth, Plymouth, UK

⁶Department of Ecology, Environment and Plant Sciences, Stockholm University, Stockholm, Sweden

⁷Centre for Natural History (CeNak), University of Hamburg, Hamburg, Germany

Correspondence

Fokje L. Schaafsma, Wageningen Marine Research, Ankerpark 27, 1781 AG Den Helder, The Netherlands.

Email: fokje.schaafsma@wur.nl

Present addresses

Giulia Castellani, Norwegian Polar Institute, Tromsø, Norway; and Julia Ehrlich, Applied Ecology and Phycology, University of Rostock, Rostock, Germany.

Funding information

Nederlandse Organisatie voor Wetenschappelijk Onderzoek, Grant/Award Numbers: 866.18.003, 866.13.009; European Commission, Grant/Award Number: EASME/EMFF/2018/1.3.2.2/03/SI2.805469; Ministerie van Landbouw, Natuur en Voedselkwaliteit, Grant/Award Number: WOT-04-009-047.04; Helmholtz Association (POF-4), work packages 6.1 and 6.3, Grant/Award Number: VH-NG-800; Bundesministerium für Bildung und Forschung (BMBF), Grant/Award Number: Grant 03F0917A MOSAiC 3; Natural Environment Research Council, Grant/Award Number: NE/S002502/1; University of Hamburg, HmbNFG,

Abstract

Polar cod (*Boreogadus saida*) is an endemic key species of the Arctic Ocean ecosystem. The ecology of this forage fish is well studied in Arctic shelf habitats where a large part of its population lives. However, knowledge about its ecology in the central Arctic Ocean (CAO), including its use of the sea-ice habitat, is hitherto very limited. To increase this knowledge, samples were collected at the under-ice surface during several expeditions to the CAO between 2012 and 2020, including the Multidisciplinary drifting Observatory for the Study of Arctic Climate (MOSAiC) expedition. The diet of immature *B. saida* and the taxonomic composition of their potential prey were analysed, showing that both sympagic and pelagic species were important prey items. Stomach contents included expected prey such as copepods and amphipods. Surprisingly, more rarely observed prey such as appendicularians, chaetognaths, and euphausiids were also found to be important. Comparisons of the fish stomach contents with prey distribution data suggests opportunistic feeding. However, relative prey density and catchability are important factors that determine which type of prey is ingested. Prey that ensures limited energy expenditure on hunting and feeding is often found in the stomach contents even though it is not the dominant species present in the environment. To investigate the importance of prey quality and quantity

See supporting information for the MOSAiC team ECO.

This is an open access article under the terms of the [Creative Commons Attribution](#) License, which permits use, distribution and reproduction in any medium, provided the original work is properly cited.

© 2024 The Author(s). *Journal of Fish Biology* published by John Wiley & Sons Ltd on behalf of Fisheries Society of the British Isles.

Grant/Award Number: 4-GLF-2017;
Expedition grants, Grant/Award Numbers:
ARK XVII/3, AWI_PS92_00,
AWI_PS106/1_2-00, AWI_PS122_00

for the growth of *B. sarda* in this area, we measured energy content of dominant prey species and used a bioenergetic model to quantify the effect of variations in diet on growth rate potential. The modeling results suggest that diet variability was largely explained by stomach fullness and, to a lesser degree, the energetic content of the prey. Our results suggest that under climate change, immature *B. sarda* may be at least equally sensitive to a loss in the number of efficiently hunted prey than to a reduction in the prey's energy content. Consequences for the growth and survival of *B. sarda* will not depend on prey presence alone, but also on prey catchability, digestibility, and energy content.

KEY WORDS

Arctic cod, bioenergetics, central Arctic Ocean, sea-ice habitat, stomach content, zooplankton

1 | INTRODUCTION

Polar cod *Boreogadus sarda* (Lepechin 1774) is an endemic key species in the ecosystem of the Arctic Ocean (Geoffroy et al., 2023). It has a circumpolar distribution, occupying shelf and slope waters, as well as the sea-ice habitat covering the deep basins of the central Arctic Ocean (CAO). The *B. sarda* associated with sea ice are usually first-year and second-year juveniles or immature individuals (Andriashev et al., 1980; David et al., 2016; Lønne & Gulliksen, 1989; Melnikov & Chernova, 2013). It has been suggested that these individuals are late hatchers that remain at the surface layer to avoid competition with larger individuals that hatch early in the season and migrate to deeper waters (Geoffroy et al., 2016). Juveniles are found to descend in the water column with increasing size, eventually joining older fish dwelling in deeper water layers or near the bottom (Benoit et al., 2014; Geoffroy et al., 2016; Matley et al., 2012). The immature *B. sarda* that remain associated with the sympagic habitat drift with the sea ice from their shelf spawning grounds into the deep basins (David et al., 2016), where they have been found in the surface waters directly in association with the sea ice (Andriashev et al., 1980; David et al., 2016; Gradinger & Bluhm, 2004; Melnikov & Chernova, 2013). *B. sarda* is one of the few fish species that occur in the CAO, and many questions regarding its distribution, habitat use, and life cycle are still unanswered (Geoffroy et al., 2023; Gradinger & Bluhm, 2004; Melnikov & Chernova, 2013; Snoeijs-Leijonmalm et al., 2020). Although there is great uncertainty regarding the abundance of this species in the CAO due to sampling difficulties, available evidence suggests that high numbers may occur in the region (Andriashev et al., 1980; David et al., 2016; Melnikov & Chernova, 2013; Snoeijs-Leijonmalm et al., 2021, 2022). The sea ice is believed to have multiple functions for *B. sarda*: a transport mechanism, a shelter from predators and/or unstable hydrodynamic conditions, and a feeding ground (David et al., 2016; Kohlbach et al., 2017; Maes et al., 2021; Melnikov & Chernova, 2013).

To date, dietary information is mainly derived from studies on *B. sarda* sampled in shelf and slope areas (e.g., Gray et al., 2016; Maes et al., 2022; Nakano et al., 2016; Renaud et al., 2012; Walkusz

et al., 2013), whereas little information is available from individuals that inhabit the sea ice-covered deep basins (Kohlbach et al., 2017; Lønne & Gulliksen, 1989; Melnikov & Chernova, 2013; Renaud et al., 2012). Recent studies indicate that fish caught underneath the ice largely prey on sympagic species, and that the majority of the carbon in their tissue originates from ice algae (Kohlbach et al., 2017; Vane et al., 2023). There is, however, hardly any knowledge about the potential geographic, seasonal, or annual variability in the diet of *B. sarda* from the CAO (Geoffroy et al., 2023; Matley et al., 2013; Snoeijs-Leijonmalm et al., 2020). Such information is essential for understanding how these fish utilize the resources of the pelagic and sea-ice habitats of this region. It is also needed to predict the consequences of climate change for population dynamics of *B. sarda* and for future fisheries management in the Arctic Ocean (Snoeijs-Leijonmalm et al., 2020).

Our limited understanding of the feeding ecology of *B. sarda* under the ice-covered Arctic Ocean can be enhanced by using numerical models, allowing scientific hypotheses to be tested with limited data available. Yet, fish feeding behavior continues to be a difficult process to model, and questions related to prey selection and foraging are particularly challenging (Fiksen & MacKenzie, 2002). To overcome these challenges, bioenergetic models with simplified foraging and feeding modules compute growth rate as a balance between food consumption (energy gain) and metabolic losses (respiration, excretion, and other losses through activity), both of which are affected by fish size and temperature (Brett, 1979; Railsback & Rose, 1999; Roy et al., 2004). Such models proved useful in predicting growth potential of fish in response to changes in prey availability and temperature (Roy et al., 2004; Thanassekos & Fortier, 2012). Using a bioenergetic model of larval *B. sarda* growth, David et al. (2022) showed that the quantity of ingested food and the energetic content of the prey explained higher variability in modeled growth than natural habitat temperature, providing further insight into feeding ecology of this fish.

The main aim of this study was to improve our knowledge on the feeding ecology of immature *B. sarda* inhabiting the sea-ice habitat of the CAO. We investigated the diet of individuals collected in the ice-

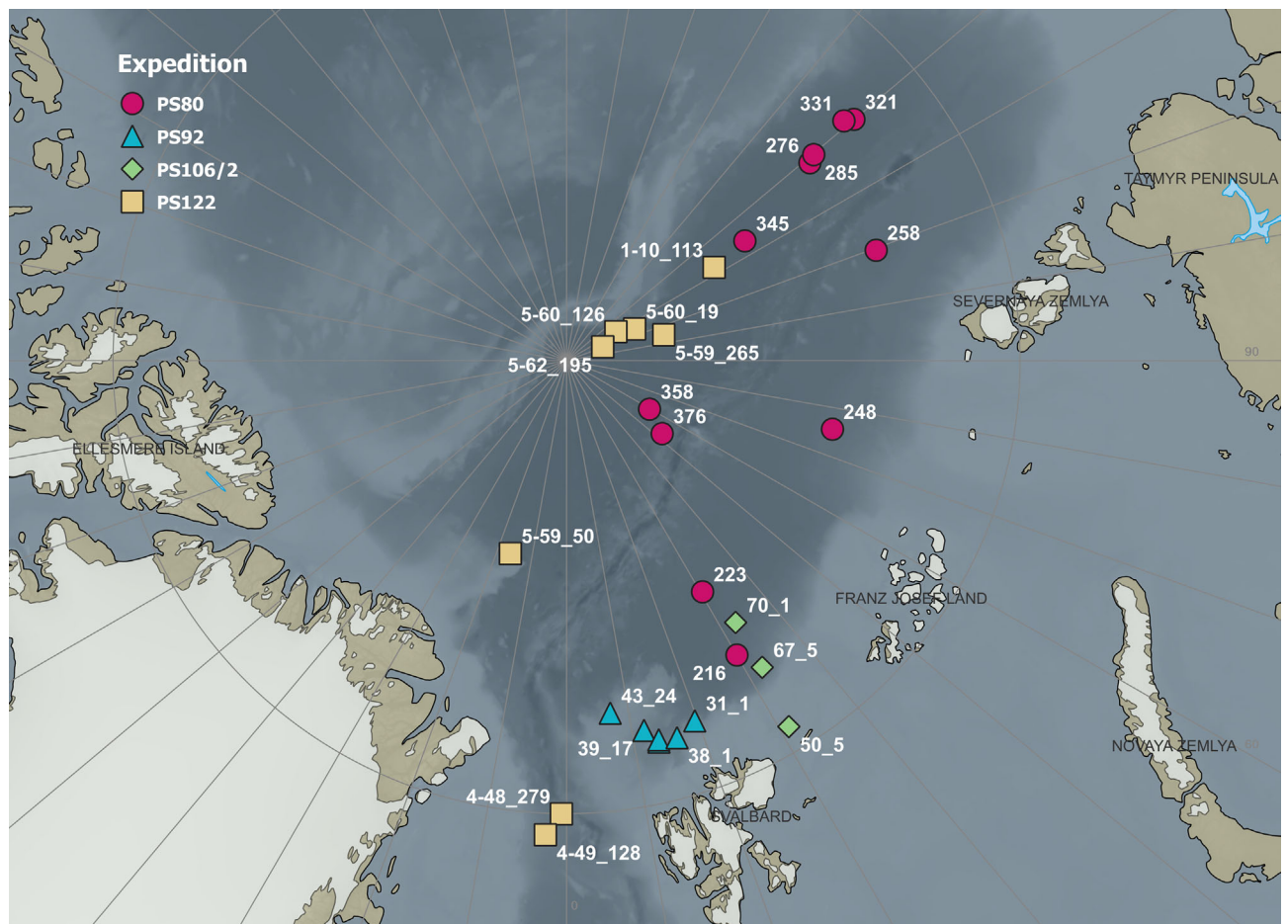


FIGURE 1 Map of the sampling area. Symbols represent sampling stations of polar cod (*Boreogadus saida*), which are color-coded based on expedition. For each expedition, the station numbers are given. Those of PS122 (MOSAiC expedition) are preceded by their respective cruise leg.

water interface during four *Polarstern* expeditions in the Arctic Ocean (PS80, previously summarized in Kohlbach et al., 2017; PS92; PS106/2; and PS122). Our objectives were to (1) provide an inventory of the stomach contents to gain information on the diet composition of immature *B. saida* and assess the variation herein and (2) to increase our knowledge on the feeding behavior of *B. saida* in the sea-ice habitat. To meet the latter objective, we investigated the spectrum and energy content of prey taxa present in the environment, analysed potential differences in diet per region or season, considered the relationship between the diet and available prey composition, and used a bioenergetic model to investigate the effect of food quantity, food quality, and temperature on growth rate potential of *B. saida*.

2 | MATERIALS AND METHODS

2.1 | *B. saida* sample collection

B. saida were sampled on board R.V. *Polarstern* (Alfred-Wegener-Institut Helmholtz-Zentrum für Polar- und Meeresforschung, 2017) using a Surface and Under-Ice Trawl (SUIT) during PS80 in the

Eurasian Basin of the CAO in late summer/autumn (August 2–October 7, 2012), north of Svalbard during PS92 in spring (May–June 2015), and north of Svalbard during PS106/2 in spring/early summer (June–July 2017). The SUIT sampled the upper 2 m of the water column in open water and under-sea ice. It consisted of a steel frame with a 2 × 2 m opening and two 15-m-long nets attached. One net was a 7-mm half-mesh shrimp net, and the other was a zooplankton net with a 300 µm (PS80, PS92) or 150 µm (PS106/2) mesh. Due to an asymmetric bridle, the net was forced to tow off at an angle allowing it to sample the surface water directly underneath sea ice, outside the ship's wake (Van Franeker et al., 2009; Flores et al., 2012). Using the SUIT, 53 individual *B. saida* were collected for diet analyses at 11 stations during PS80 (Kohlbach et al., 2017), 12 individuals at 6 stations during PS92, and 5 individuals at 3 stations during PS106/2 (Figure 1).

B. saida were also collected during PS122 (MOSAiC expedition) on board R.V. *Polarstern*, which took place from September 20, 2019, to October 12, 2020. The expedition was subdivided into five legs. Four legs took place starting from the initial deployment in late September 2019 north of the Laptev Sea, then drifting south within the Transpolar Drift, and ending in Fram Strait in July 2020. The ice

station was relocated for the fifth leg to near the North Pole in August 2020, where it remained until the end of the expedition in late September 2020. In total, 16 *B. saida* suitable for diet studies were collected from underneath the ice during Legs 1, 4, and 5 (Figure 1). One fish was collected in winter during Leg 1 (December 7, 2019) with a remotely operated vehicle (ROV) operating at 10 m depth on December 7, 2019. Most specimens ($n = 9$) were collected in a single sampling event on July 25, 2020, during Leg 4 (June 4–August 12, 2020), using Castellani's stick-and-scoop method. This method consisted of using a long thin stick to gently disturb the fish in a crack from the bottom of the crack so that they moved toward the surface, where they were scooped out of the water by hand. The method proved to be very successful when *B. saida* were residing in narrow cracks in the ice where no net can be used. Six more individuals were caught in the period between end of July and mid-September 2020. During Leg 5 (August 12–October 12, 2020), *B. saida* were caught with hand-held sieves or a ring net from holes in the ice and sampled unintentionally by the ship's seawater intake.

2.2 | Fish stomach content analysis

Fish were dissected either directly on board or in the home laboratories after they had been preserved frozen at -20°C . The total length (L_T), standard length (L_s), and wet mass (M_W) of the fish were recorded before dissection. Stomachs were preserved in 96% ethanol. After dissection, the eviscerated wet mass (W_{ev}) of the fish was recorded. To investigate whether there were differences in the condition of the fish among expeditions, the Fulton's condition index K per individual fish in percentage was calculated as follows:

$$K = 100 \times M_W / L_T^3 \quad (1)$$

After the stomachs were weighed, they were cut open, and the contents were rinsed from the stomach into a Petri dish or a Bogorov counting chamber with deionized water. The empty stomachs were weighed again to calculate stomach content mass (M_{Sc}). Prey items in the stomach content were identified to the lowest possible taxonomic level and counted using a Discovery V8 stereomicroscope (Zeiss, Germany). Identification to species level was possible only when species-specific features were still present. Often, specimens could only be identified to higher taxonomic levels, such as "copepods" or "amphipods." These groups may, consequently, include individuals of species that were also presented separately. Identifiable body parts were counted, and, together with whole animals, used to estimate the minimum number of individuals (MNI) of each prey taxon in each fish stomach. Separate body parts were assumed to belong to a single individual unless there was evidence indicating otherwise, for example, when several copepod urosomes or amphipod telsons were present.

Size measurements of the prey items were performed using an AxioCam HRc with AxioVision40 V 4.8.2.0 software (Zeiss, Germany).

When possible, the L_T of gammarid amphipods were measured from the tip of the rostrum to the tip of the telson (in millimeters) and from the front of the head to the tip of the telson for hyperiid amphipods. When animals were broken, either head length or telson length was recorded to be able to reconstruct the L_T (Schaafsma et al., 2022). The prosome length (L_P) and urosome length (L_U) of copepods were measured when possible. For appendicularians, the maximum length of the trunk (L_{TR}) was measured (Aguirre et al., 2006). When no length measurements were possible, due to digestion, the best available alternative for a size estimate of consumed prey was used, such as the L_T of specimens collected in the field or measurements performed on stomach content of fish collected during other expeditions (Table 1).

Reconstructed biomasses of all identifiable food items in the stomach were estimated by multiplying the minimum number of individuals of a species with the mean reconstructed individual dry mass (M_D in milligram individual $^{-1}$). The M_D was estimated from L_T , L_P , or L_{TR} (Table 1) using regression models developed from measurements on individuals that were collected during the expedition on which the fish was caught, during other expeditions (Schaafsma et al., 2022), or derived from literature when such models were not available from our own measurements. For a few taxa, no regression models were available, and a model for a closely related group or dry mass estimates derived from literature were used. An overview of mean dry masses used, including sources used for estimation, is presented in Table S1.

The frequency of occurrence (F_O) of prey items per expedition was calculated by dividing the number of fish stomachs that contained a certain prey item by the total number of stomachs analysed from that expedition, and then multiplying by 100 to express the value as a percentage. For each expedition, the index of relative importance (I_{RI}) of the prey items was then calculated, using mass instead of volume (Hacunda, 1981; Liao et al., 2001; Pinkas et al., 1971), as follows:

$$I_{RI} = (A + B) \times F_O \quad (2)$$

where A is the mean relative abundance (in percentage) of the prey item in the stomachs, B is the mean relative biomass (in percentage) of the prey item in the stomachs, and F_O is the frequency of occurrence (in percentage) of the prey item in the stomachs. The percentage I_{RI} for each prey item per expedition was then calculated by dividing the I_{RI} of a prey item by the sum of that I_{RI} of all prey items found during that expedition and multiplying it by 100.

Because the state of the digestion of the prey in the stomach can influence the number and size of prey that can be reconstructed and may hamper comparisons among diets, a degree of digestion (D_D) between 1 and 4 was assigned, with 1 = undigested, 2 = partially digested, 3 = advanced digestion, and 4 = almost complete or complete digestion. Large differences in D_D among groups of fish investigated can help to assess whether differences in the diet were influenced by this factor.

TABLE 1 Average total length (in millimeters) or prosome length (L_p in millimeters) of taxa found in the stomach contents of polar cod (*Boreogadus saida*) used for prey size comparisons and biomass reconstruction.

Prey item	Expedition			
	PS80	PS92	PS106/2	PS122
Copepod UNID (L_p)	2.46 (n = 28)	2.60 (n = 110)	3.76 (n = 19)	3.26 (n = 27)
Harpacticoid UNID	2.11 (n = 1)			
<i>Calanus</i> spp. (L_p)	2.46 (n = 28)	2.55 (n = 101)	3.76 (n = 19)	3.40 (n = 19)
<i>Pseudocalanus</i> spp.		1.00 ^a		
<i>Paraeuchaeta</i> spp. (L_p)	4.00 (n = 1)	6.81 (n = 1)		4.36 (n = 1)
<i>Metridia</i> sp. (L_p)		2.67 (n = 6)		
<i>Tisbe</i> sp. (L_p)	0.63 (n = 83)			
Amphipod UNID	8.88 (n = 44)			
<i>Apherusa glacialis</i>	8.81 (n = 30)	9.68 ^b	11.54 ^b	5.40 (n = 2)
<i>Themisto</i> spp.	6.90 (n = 6)	14.72 ^b		6.39 (n = 1)
Euphausiids UNID			23.59 ^b	
<i>Thysanoessa</i> spp.			23.59 ^b	
Decapod	NA			
Appendicularians	2.48 ^c	3.54 (n = 2)		2.45 (n = 62)
Chaetognaths	21.26 ^d	21.26 ^b		21.26 ^d

Note: Averages were based on measurements performed directly on the stomach contents unless indicated otherwise. Averages of unidentified species groups (copepod UNID, amphipod UNID, and krill UNID) were based on all measurements available in that group. For copepods, measurements per expedition were used, whereas for amphipods, measurements from all expeditions were pooled.

n = number of individuals measured in the stomachs.

^aEstimated from Hopcroft and Kosobokova (2010).

^bMeasured on zooplankton samples from the environment collected during the respective expedition.

^cAverage of measurements of all specimen from PS92 and PS122.

^dMeasured on samples from the environment collected during PS92.

2.3 | Zooplankton sample collection for community structure analysis

During PS122, the zooplankton community directly underneath the sea ice was sampled using a plankton net attached to a ROV (ROV net; Wollenburg et al., 2020), operated through a hole in the ice at approximately 500-m distance from R.V. *Polarstern*. The ROV net had an opening of 0.24 m² and was equipped with a 150-μm mesh. Immediately after sampling, the zooplankton samples were transferred to small barrels, which were placed in cooling boxes, to prevent freezing during the transport to the ship. Onboard, the samples were preserved in 4% formaldehyde-seawater solution, buffered with hexamethylenetetramine, and stored at room temperature until further processing. The zooplankton community structure was analysed using the ZooScan (Biotom, Hydroptic, France) following the procedure described by Gorsky et al. (2010). This method allowed us to determine Arctic zooplankton species at a taxonomic level that is similar to that of microscopy (Cornils et al., 2022). Briefly, all samples were size-fractionated using 1000- and 500-μm meshed sieves to facilitate semiautomatic image analyses. The three size fractions were split using a Folsom plankton splitter into aliquots not smaller than 1/16 and subsequently scanned with a resolution of 2400 dpi using VueScan (version 8.3.23). Before each scan, air bubbles were removed, and overlapping individuals were separated using forceps. The scans were processed with ZooProcess (version 7.19), yielding images with single objects linked to associated metadata.

Images and metadata were then uploaded to the EcoTaxa server (<https://ecotaxa.obs-vlfr.fr>). Based on our training sets from previous Arctic expeditions, categories for all objects were predicted using random forest and deep-learning algorithms provided by EcoTaxa. These predictions were manually validated, yielding the number of organisms in each aliquot. Abundance data (individual m⁻³) were then calculated based on the distance that the ROV covered during the haul and the net opening. The zooplankton community of PS106/2 was sampled at the ice–water interface using a ROV net (5 m length, 0.5-mm mesh) with a similar net opening of 0.24 m² (Flores et al., 2018). Zooplankton samples were directly preserved on a 4% hexamine-buffered formaldehyde-seawater solution until further processing with a M205 C stereomicroscope (Leica, Germany). On expeditions, PS80 (David et al., 2015) and PS92 (Ehrlich et al., 2020) zooplankton were collected simultaneously with *B. saida* using the SUIT. Similar to PS106/2, the catch was preserved on a 4% hexamine-buffered formaldehyde-seawater solution until enumeration with a stereomicroscope.

2.4 | Zooplankton sample collection for energy content

Zooplankton samples for energy content measurements were collected during PS122 over various depth intervals either with vertical tows using ring nets (0.79-m² net opening) equipped with 53-, 150-,

or 1000- μm mesh, a Nansen net (0.38- m^2 net opening) equipped with 150- μm mesh, or with horizontal tows using the ROV net towed at 0, 10, or 95 m depth. After collection, the samples were brought to the laboratory on board, where various taxa (Amphipoda, Chaetognatha, Euphausiacea, *Calanus hyperboreus*) were sorted from the samples using forceps. The specimens were briefly rinsed in MilliQ water to remove salt, transferred to Eppendorf tubes, and then stored at -20°C until further analysis. An overview of PS122 samples used for energy content estimates, including details of sampling, can be found in Table S2. During PS92, individuals for energy content analysis were collected from the SUIT net catch before the remainder of the sample was stored for community structure analysis. A few samples for energy content analysis were collected from deeper water layers using a rectangular midwater trawl (RMT 8 + 1 with 4.5- and 0.33-mm mesh).

2.5 | Energy content measurements

The M_W and, where possible, L_T of zooplankton for energy content estimates were measured after thawing. The L_T of chaetognaths could not be established as they were broken or deformed. After thawing, the samples were freeze-dried until complete desiccation to determine the M_D of the animals. During freeze-drying, samples consisted mainly of single individuals. In some cases, when it was clear up front that individuals needed to be pooled for energy content measurements, a sample consisted of pooled individuals. The energy content of prey species was then measured using a 6725 semimicro oxygen calorimeter (Parr, USA) connected to a 6772 calorimetric thermometer (Parr, USA). Animals were pressed into sample pills using a 2817 (1/4" diameter) pellet press (Parr, USA). When the M_D of the specimens was <0.1 g, the sample was supplemented with standardized benzoic acid powder until a total weight of approximately 0.2 g was reached. Benzoic acid has a fixed calorific content of 6318.4 cal g^{-1} (26.453 kJ). Some animals were even smaller and had a M_D of <0.01 g. In such cases, individual animals were pooled to reach a sample weight of at least 0.015 g, as trial measurements revealed that lower sample weights may yield unrealistic results. Benzoic acid was also added to these samples to reach approximately 0.2 g. After the measurement, the calorific content was corrected for the combustion of fuse wire and benzoic acid when necessary. To compare among or within prey species, the energy density is expressed as $\text{kJ g}^{-1} M_D$, calculated using a conversion factor of 1 cal = 4.1868 J, whereas for studying the growth rate potential of *B. saida*, the energy density in cal $\text{g}^{-1} M_W$ was used (Båmstedt, 1986; Schaafsma et al., 2018). The energy content was measured in the copepod *C. hyperboreus*, the amphipods *Apherusa glacialis*, *Themisto abyssorum*, and *Themisto libellula*, the krill *Thysanoessa longicaudata*, and chaetognaths.

2.6 | Environmental parameters

During PS122, quality-controlled daily sea-surface temperature (SST) and salinity were provided (Schulz et al., 2023) from various

conductivity temperature depths (CTDs) (Hoppmann et al., 2022; Tippenhauer et al., 2023a, 2023b; Schulz et al., 2022). We used temperature recorded during the time spent at the respective station (Rabe et al., 2022). Values of satellite sea-ice concentration in a 3-km radius around the research vessel were obtained as in Krumpen et al. (2021). On expeditions PS80, PS92, and PS106/2, sensors mounted on the SUIT frame collected environmental data during trawling. Water temperature, salinity, and depth were measured using a CTD probe (Sea and Sun Technology CTD75M memory probe). Satellite data were used to calculate sea-ice concentration (in percentage) in the area. Details on the methods and all environmental data of these expeditions can be found in Castellani et al. (2020).

2.7 | Predictors of growth rate

A bioenergetic model (David et al., 2022) was used to simulate daily growth rates of *B. saida* based on the stomach fullness and prey content at the moment of capture. The model simulated temperature- and food-dependent growth rates (GR, in $\text{g g}^{-1} \text{ day}^{-1}$) as the energy gained through food consumption minus the energy lost through respiration and other metabolic processes through the general energy-balance equation:

$$\text{GR} = P \times C_{\max} \times A - R \times (SDA + f_{\text{act}}) \quad (3)$$

where P is the fraction of the maximum mass-specific consumption C_{\max} , A ($= 0.8$) is the assimilation efficiency, representing the remaining consumption after egestion and excretion, R is the basal respiration rate, SDA ($= 0.375$) is the specific dynamic action representing the metabolic increase due to digestion, and f_{act} ($= 1.5$) is the increase due to activity. The equations for consumption (C_{\max}) and respiration (R) were expressed as a function of fish mass and temperature (Text S1; David et al., 2022) and were determined in laboratory experiments with juveniles (Hop et al., 1997; Hop & Graham, 1995). The metabolic processes were described by weight-specific equations, which make the model applicable to a range of fish weights from larvae to immature fish. The model was validated for larvae and age-0 juveniles by David et al. (2022) and for older juveniles age +1 and +2 against experimental data of Kunz et al. (2016) (Figure S1). The surface water temperature, at the moment the fish were sampled, was used as the input temperature. In the model, daily ration was expressed as a fraction of C_{\max} , mediated through the parameter P , which in this context is equivalent to stomach fullness. For each fish, P was calculated as the ratio between the stomach content mass (wet mass in grams) and a theoretical maximum stomach content mass, assumed per fish weight class intervals of 1 g. The maximum stomach content mass per weight class intervals was theoretically assumed using a third-degree polynomial function fitted to the upper value of all measured stomach content masses (Figure S2). To express the conversion efficiency from ingested prey to fish tissue, the model uses a ratio between energetic content of ingested prey and energetic content of *B. saida* (David et al., 2016; David et al., 2022). The total energetic content of ingested prey for each individual fish was

estimated using the percentage of species/taxonomic group contribution to stomach content M_W multiplied with their energetic content in $\text{cal g}^{-1} M_W$. To estimate the percentage M_W contribution of each prey category, the M_W s of the prey items found in the stomach content were reconstructed based on the number of recognizable food items, and percentages were calculated as a fraction of the sum of all reconstructed M_W s. This approach minimizes the underestimation of the contribution of fast-digesting tissue to the diet (e.g., appendicularian bodies). The M_W and energy content per prey item used can be found in Tables S2 and S3, respectively. The relative importance of stomach fullness (P), energetic content of ingested prey, and temperature to the modeled growth rates was assessed with a linear regression model and calculated with a bootstrap method using the R library “relaimpo” (Grömping, 2006).

2.8 | Statistical analysis

Differences in L_T , M_W , and K of the fish, and M_{SC} and D_D of the stomach contents of the fish among expeditions, as well as differences in energy content among more than two groups within a species, were analysed using an ANOVA followed by a non-parametric Tukey honestly significant difference (THSD) test. Differences between two groups were analysed using the non-parametric Wilcoxon rank-sum test. The statistical significance level α was set at 0.05.

A hierarchical agglomerative cluster analysis based on a Manhattan distance matrix and group-average linkage was performed to investigate if there were natural groupings in the diet composition indicating if the stomach contents of fish were more similar within, for example, a region or sampling season than those from other regions or sampling seasons (Clarke & Warwick, 2001; Greenacre, 2017). The diet data were expressed in percentages per individual fish to focus the analysis on relative differences between diet composition rather than between numbers of prey items (Greenacre, 2017). Data from stomachs with fewer than five recognizable food items were removed from the analysis to avoid unrealistic relative characterizations of the diet composition. Statistical analyses and concomitant visualization of results were performed in R version 4.2.1 (R Core Team, 2022) using packages “vegan” (Oksanen et al., 2020), “dendextend” (Galili, 2015), and “ggplot2” (Wickham, 2015).

To investigate the relationship between the diet of the fish and the available prey, Ivlev's electivity index E_i was calculated as follows:

$$E_i = (r_i - p_i) / (r_i + p_i) \quad (4)$$

where r_i is the average relative abundance of food category i in the stomach, and p_i is the average relative abundance of this prey in the environment (Ivlev, 1961). E_i values range from -1 to 1, with negative values indicating selection against or inaccessibility of the prey, 0 indicating random feeding and positive values indicating active selection. The index provides rank order comparisons between food types rather than a quantitative comparison (Jacobs, 1974) and assumes that all prey types have the same possibility of being

encountered or ingested (Deudero & Morales-Nin, 2001). The index was not calculated for values of p or $r < 0.3$, as calculated electivity with such values are expected to be erroneous, and the index does not effectively assesses rare food types (Lechowitz, 1982). To further evaluate the influence of the effect of species' densities and densities of alternative prey species, the ratios between dominant prey species were assessed for areas in which the species were dominant in the *B. sarda*'s diet, as obtained from the cluster analysis.

2.9 | Ethics statement

Polar cod were sampled and processed according to and within laws, guidelines, and policies of the German Animal Welfare Organization. No specific permissions were required. The fish collected are neither endangered nor protected in the central Arctic waters and coastal waters of the Svalbard Archipelago. Polar cod were killed immediately after collection.

3 | RESULTS

3.1 | Environmental variables and fish parameters

SSTs were always below 0°C and fairly similar during sampling events. During the spring expeditions PS92 and PS106/2 (Table 2), SSTs were, on average, -1.7°C and -1.8°C, respectively, while slightly higher average temperatures were encountered during the summer/autumn seasons of PS80 and PS122, with the widest range of temperatures occurring during PS80 (-1.82 to -1.06°C). During PS122, the lowest surface water temperature of -1.79°C was found in December 2019, and the highest was found in July 2020 (-1.35°C). During the relocation of the expedition to a new floe near the North Pole in mid-August, temperatures dropped to -1.58°C. Sea-surface salinity was, on average, lower during the summer/autumn expeditions compared to the spring expeditions (Table 2). Salinities during spring were mostly >33. Lowest salinities of around 30 were encountered during PS80, particularly in the easternmost stations of the Amundsen basin. Salinity in December (PS122) was comparable to the higher end of the range of observed summer values. All fish were collected over the deep basins of the CAO during PS80 and PS122, whereas a few stations were situated on the slopes of Svalbard's continental shelf during PS92 and PS106/2.

The fish collected during PS80 were significantly smaller than those collected during the other expeditions (ANOVA L_T : $F_{3,81} = 17.83$, $p < 0.0001$; THSD $p < 0.001$; Table 3). The size frequency distribution of collected *B. sarda* can be found in Figure S3a. Mean fish M_W ranged between 3.4 g on PS80 and 20.8 g on PS106/2 and differed significantly among all expeditions (ANOVA $F_{3,71} = 19.74$, $p < 0.004$; THSD $p < 0.003$), except between PS92 and PS122. The mean condition index K did not significantly differ among expeditions (Table 3). There were also no significant differences in D_D of the food in the stomachs among expeditions. The M_{SC} were

TABLE 2 Summary of environmental variables at stations where polar cod (*Boreogadus saida*) were sampled.

Expedition	Sampling period	Average surface temperature (°C) ± SD	Average salinity	Bottom depth (m) range	Average (satellite-derived) sea-ice coverage (%) ± SD
PS80	Aug. 7–Sept. 25, 2012	−1.49 ± 0.22	31.32 ± 1.34	3423–4384	53.8 ± 23.4
PS92	June 3–19, 2015	−1.79 ± 0.06	33.75 ± 0.24	794–2139	98.6 ± 3.2
PS106/2	June 29–July 5, 2017	−1.74 ± 0.04	33.72 ± 0.32	104–3810	92.7 ± 3.7
PS122/4–5 (s/a)	July 15–Sept. 19, 2020	−1.64 ± 0.12	32.12 ± 2.02	2508–4320	86.9
PS122/1 (w)	Dec. 7, 2019	−1.76	32.34	4398	90.0

Note: The data for PS122 summer/autumn (s/a) and winter (w) are presented separately.

TABLE 3 Summary of parameters of polar cod (*Boreogadus saida*) collected for stomach content analysis during four expeditions in the central Arctic Ocean.

Expedition	n	L_T (mm)	L_S (mm)	M_W (g)	K	D_D	M_{Sc} (g)
PS80	53	78.5 ± 18.5	71.7 ± 16.9	3.44 ± 3.06	0.63 ± 0.08	3.08 ± 0.86	0.09 ± 0.09
PS92	12	105.8 ± 26.4	96.6 ± 24.0	9.30 ± 6.77	0.65 ± 0.08	3.42 ± 0.67	0.45 ± 0.62
PS106/27	5	122.0 ± 25.2	112.4 ± 21.5	20.80 ± 5.52	0.72 ± 0.09	3.20 ± 0.84	1.14 ± 1.05
PS122/4–5 (s/a)	15	111.1 ± 18.7	100.2 ± 17.2	9.49 ± 4.54	0.66 ± 0.06	2.89 ± 0.94	0.13 ± 0.13
PS122/1 (w)	1	106.0	97.0	6.00	0.50	4	0.01

Note: Averages and SDs of fish total length (L_T), fish standard length (L_S), fish wet mass (M_W), fish condition index (K), degree of digestion of stomach contents (D_D), and the mass of stomach content (M_{Sc}) are presented. Data collected during PS122 summer/autumn (s/a) and winter (w) are presented separately.

significantly different among most expeditions (ANOVA $F_{3,64} = 16.12$, $p < 0.03$; THSD $p < 0.02$; Table 3), but not between PS80 and PS122, and between PS92 and PS122. The stomach contents of fish collected during PS106/2 were significantly heavier than those of fish collected during the other expeditions (THSD $p < 0.004$).

3.2 | Diet of *B. saida* from the central Arctic Ocean

The number of identifiable prey items per individual was usually fewer than 100 in all expeditions, with a few exceptions (up to >1200 individuals) during PS92 and PS106/2. The stomach contents of *B. saida* caught during three expeditions were numerically dominated by copepods. *Calanus* spp. numerically dominated the diet during the two spring expeditions (PS92 and P106/2), whereas the harpacticoid *Tisbe* sp. dominated during late summer/autumn (PS80; Kohlbach et al., 2017) followed by *Calanus* spp. (Figure 2). In terms of M_D , *Calanus* spp. was also the dominant food item during expeditions PS92 and PS106. During PS80, M_D of the stomach contents were dominated by the ice-associated amphipod *A. glacialis* (Table 4). High numbers of amphipods were found in the stomachs of fish collected only during this expedition. Appendicularians were not common in the stomachs of fish from expeditions other than PS122. They accounted for 1.3% of the total recognizable food items in fish from PS92, although with a relatively high F_O . Chaetognaths were also a relatively common

food item during expedition PS92, occurring in 66.7% of the stomachs, albeit in low numbers. Krill (Euphausiidae) were only found in the stomach contents of fish collected during PS106/2 (Figure 2; Table 4). During PS80, 27.5% of the stomachs were infested with the trematode parasite *Hemiurus levinseni* (Kohlbach et al., 2017), which is usually hosted by calanoid copepods (Køie, 2009). No parasites were found in the stomachs of fish from PS92. From the fish of PS106/2, one stomach contained two trematode parasites, and one stomach contained a single nematode parasite.

Identifiable prey items in *B. saida* stomachs from PS122 were limited to four taxonomic groups, namely copepods (62.5% F_O), appendicularians (56.3% F_O), chaetognaths (42.8% F_O), and amphipods (25% F_O). Two of the 16 individuals had empty stomachs, in one of which a trematode parasite was found. On average, appendicularians numerically dominated the diet of *B. saida* during the summer/autumn months (PS122/4–5) of PS122 (53.8%) followed by copepods (17.9%; Figure 2), whereas copepods, appendicularians, and chaetognaths dominated the diet in terms of M_D (30.5%, 30.5%, and 20.9%, respectively; Table 4). Identifiable copepods consisted mainly of the genus *Calanus* (Table 4). Of the amphipods, *A. glacialis* and *T. abyssorum* could be identified to species level. The stomach of the single winter individual, collected during PS122, contained little food (Figure 2; Table 4), and the few food items that were recognizable comprised 80% copepods and 20% chaetognaths numerically.

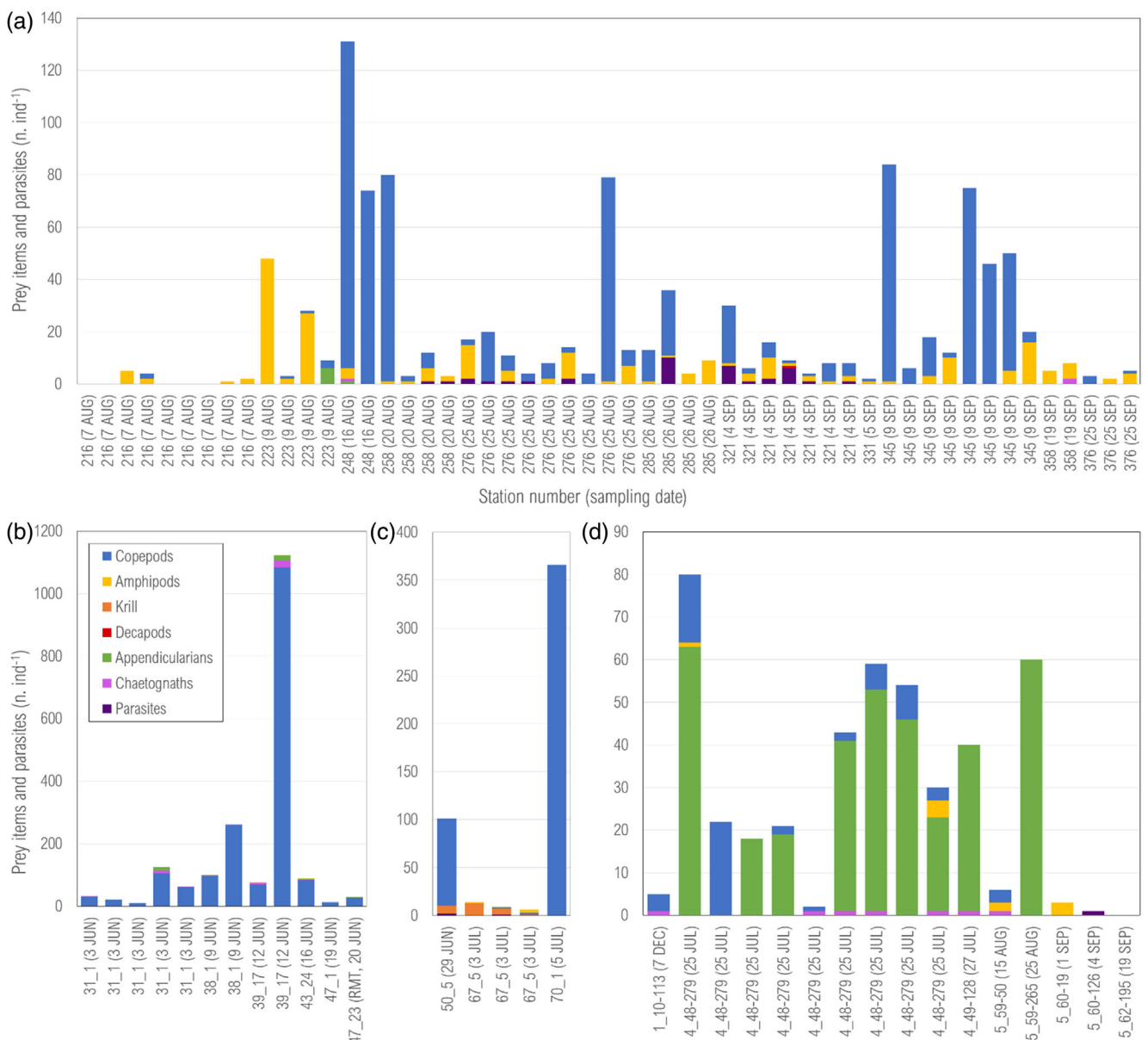


FIGURE 2 Stomach content of individual polar cod (*Boreogadus saida*) from the central Arctic Ocean. Each individual fish is indicated by its sampling station and catch date (in brackets) on the x-axis. The fish were collected during expeditions PS80 (a, previously summarized in Kohlbach et al., 2017), PS92 (b), PS106/2 (c), and PS122 (d). Prey items are the estimated minimum number of individuals (MNI) per taxonomic group. Note different scaling of the y-axis.

The I_{RI} (Figure 3) indicated that amphipods (I_{RI} : 70.5%) and copepods (I_{RI} : 29.3%) dominated by the species *A. glacialis* and *Tisbe* sp. were the most important food items during PS80 (Kohlbach et al., 2017). Copepods (I_{RI} : 92%), dominated by *Calanus* spp., were the most important food item during PS92. During PS106/2, copepods (I_{RI} : 49.9%), again dominated by *Calanus* spp., were most important, followed by euphausiids, including *Thysanoessa* sp. (I_{RI} : 45.8%). Appendicularians were the most important food item for *B. saida* during the summer of PS122 (I_{RI} : 59.0%) followed by copepods (I_{RI} : 25.7%) and chaetognaths (I_{RI} : 11.4%). Detailed I_{RI} on the lowest identified taxonomic levels can be found in Table 4.

Calanus spp. in *B. sarda* stomachs from PS80 and PS92 had L_P s of 1.5–4 mm. Some were staged as adult females (PS80), and as CIV/CV copepodites and adult females (PS92). This suggests that they belonged to either the species *Calanus finmarchicus* or *Calanus glacialis* (Madsen et al., 2001). In stomachs from fish collected at station 47_23 (PS92), adult female *Calanus* sp. with $L_P > 6$ mm were also found, which is equivalent to the size of female *C. hyperboreus* (Madsen et al., 2001). The individuals from PS106/2 stomachs were almost all adult females, and the L_P of these females suggested that the species was *C. glacialis* (Madsen et al., 2001). A wide range of *Calanus* spp. L_P s was found during PS122 (1.5–6.4 mm) and, although

TABLE 4 Average stomach contents of polar cod (*Boreogadus saida*) during four expeditions.

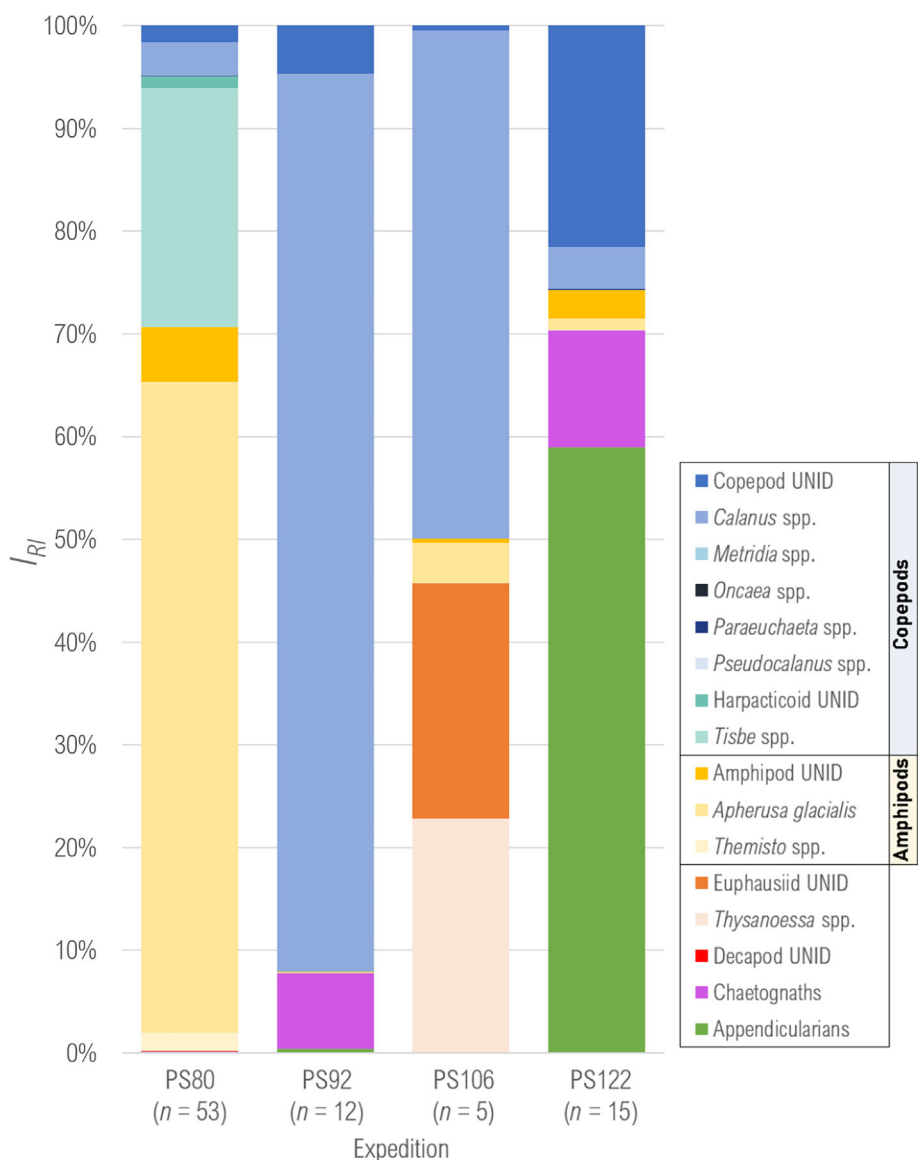
	PS80	PS92	PS106/2	PS122/4-5 (s/a)	PS122/1 (w)
<i>n</i>	53	12	5	15	1
Prey item	Average M_D stomach ⁻¹ (%) \pm SD				
Copepod UNID	4.2 \pm 14.6	7.4 \pm 15.6	1.7 \pm 3.8	17.23 \pm 25.55	44.2
Harpacticoid UNID	0.3 \pm 2.0	0	0	0	0
<i>Calanus</i> sp.	4.9 \pm 17.6	71.1 \pm 27.8	40.1 \pm 39.2	7.89 \pm 16.8	0
<i>Pseudocalanus</i> sp.	0	0.0 \pm 0.01	0	0	0
<i>Paraeuchaeta</i> sp.	1.9 \pm 13.7	0.4 \pm 1.3	0	1.3 \pm 5.2	0
<i>Metridia</i> sp.	0	0.5 \pm 1.7	0	0	0
<i>Oncaea</i> sp.	0.0 \pm 0.02	0	0	0	0
<i>Tisbe</i> sp.	8.3 \pm 25.7	0	0	0	0
Amphipod UNID	10.8 \pm 25.8	0.6 \pm 2.2	0.3 \pm 1.0	8.4 \pm 19.2	0
<i>Apherusa glacialis</i>	52.7 \pm 43.2	1.7 \pm 6.0	2.3 \pm 19.7	6.7 \pm 25.8	0
<i>Themisto</i> sp.	4.1 \pm 13.3	0.4 \pm 1.5	0	0.5 \pm 2.1	0
Euphausiid UNID	0	0	33.0 \pm 29.1	0	0
<i>Thysanoessa</i> sp.	0	0	21.4 \pm 21.9	0	0
Decapods	1.9 \pm 13.7	0	0	0	0
Chaetognaths	0.6 \pm 3.7	17.4 \pm 18.2	0	18.1 \pm 27.0	55.8
Appendicularians	0.8 \pm 5.6	0.5 \pm 0.7	0	26.5 \pm 33.7	0
F_O (%)					
Copepod UNID	18.9	50.0	20.0	53.3	
Harpacticoid UNID	20.8	0	0	0	
<i>Calanus</i> sp.	20.8	100.0	80.0	33.3	
<i>Pseudocalanus</i> sp.	0	8.3	0	0	
<i>Paraeuchaeta</i> sp.	1.9	8.3	0	6.7	
<i>Metridia</i> sp.	0	8.3	0	0	
<i>Oncaea</i> sp.	1.9	0	0	0	
<i>Tisbe</i> sp.	49.1	0	0	0	
Amphipod UNID	24.5	8.3	20.0	20.0	
<i>Apherusa glacialis</i>	64.2	8.3	40.0	6.7	
<i>Themisto</i> sp.	17.0	8.3	0	6.7	
Euphausiid UNID	0	0	60.0	0	
<i>Thysanoessa</i> sp.	0	0	80.0	0	
Decapods	1.9	0	0	0	
Chaetognaths	3.8	66.7	0	40.0	
Appendicularians	3.8	41.7	0	60.0	
I_{RI} (%)					
Copepod UNID	1.6	4.7	0.5	21.5	
Harpacticoid UNID	1.2	0	0	0	
<i>Calanus</i> sp.	3.2	87.3	49.4	4.1	
<i>Pseudocalanus</i> sp.	0	0.0	0	0	
<i>Paraeuchaeta</i> sp.	0.1	0.0	0	0.1	
<i>Metridia</i> sp.	0	0.0	0	0	
<i>Oncaea</i> sp.	0.0	0	0	0	
<i>Tisbe</i> sp.	23.2	0	0	0	
Amphipod UNID	5.4	0.0	0.4	2.8	
<i>Apherusa glacialis</i>	63.4	0.1	3.9	1.1	

TABLE 4 (Continued)

	PS80	PS92	PS106/2	PS122/4-5 (s/a)	PS122/1 (w)
<i>Themisto</i> sp.	1.7	0.0	0	0.1	
Euphausiid UNID	0	0	22.9	0	
<i>Thysanoessa</i> sp.	0	0	22.9	0	
Decapods	0.1	0	0	0	
Chaetognaths	0.1	7.4	0	11.4	
Appendicularians	0.1	0.4	0	59.0	

Note: Presented are averages of relative contribution to dry mass (M_D) and SDs, frequency of occurrence (F_O), and index of relative importance (I_{RI}). Note that many unidentified copepods likely also belong to the genus *Calanus*, which would influence the F_O and I_{RI} . For PS122, winter (w) and summer/autumn (s/a) fish were separated. For the winter fish, F_O and I_{RI} were not calculated as only one fish was caught during this season. n = the number of fish analysed from each expedition.

FIGURE 3 The importance of prey in the diet of polar cod (*Boreogadus saida*) during four expeditions, expressed as percentage index of relative importance (% I_{RI}). The PS122 data show the importance of prey items in summer/autumn. n represents the number of fishes analysed. The stomach content of the single fish caught during winter (containing small numbers of copepods and a chaetognath) was excluded from this summary. UNID, further unidentified species.



not further determined, this suggests the presence of multiple species, including *C. hyperboreus*. The size frequency of *Calanus* spp. from the stomach contents can be found in Figure S3b.

The cluster analysis separates the fish into four groups distinguished by the food items that were numerically dominant in the stomach contents: calanoid copepods (mainly *Calanus* spp.), krill,

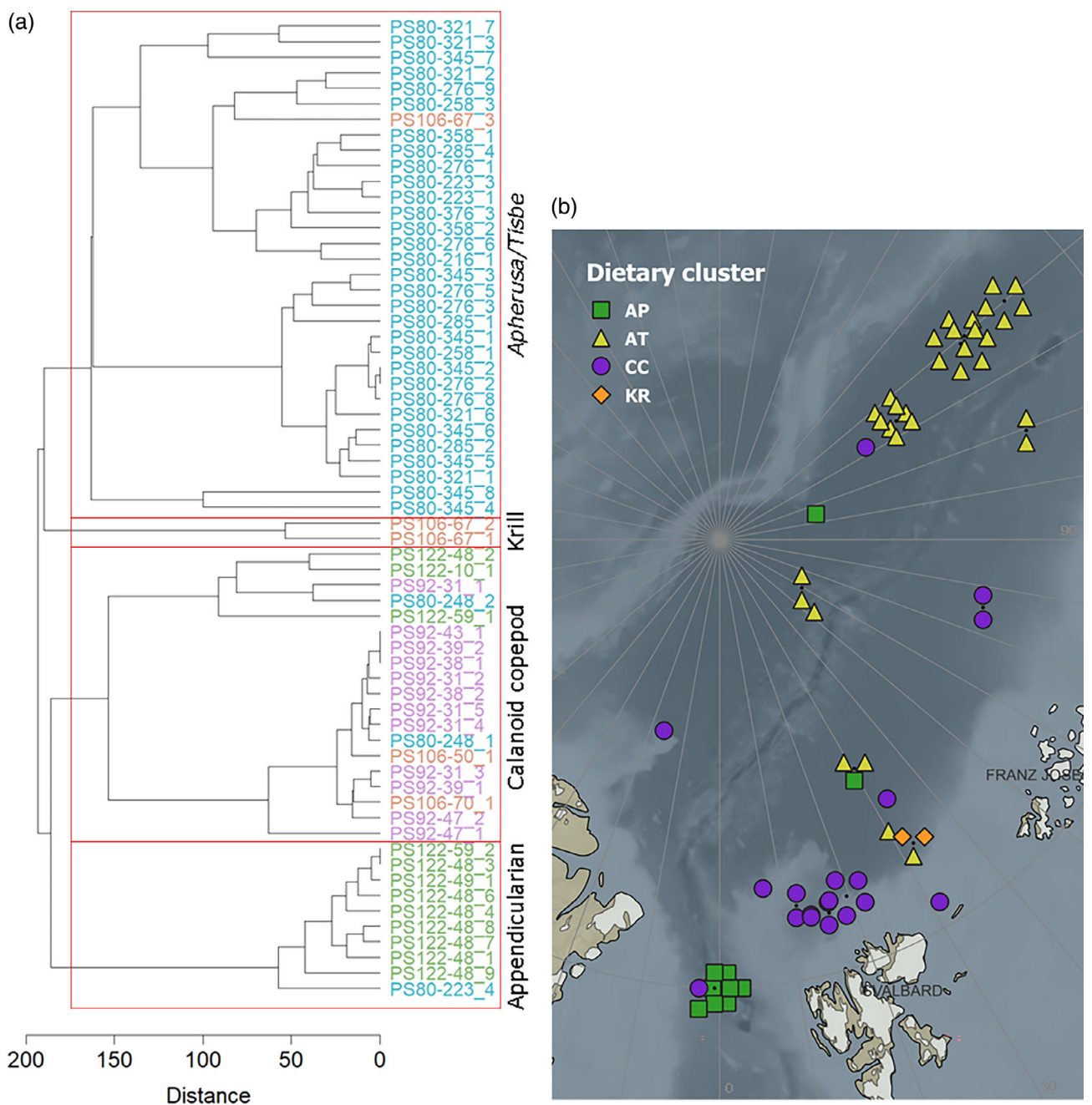
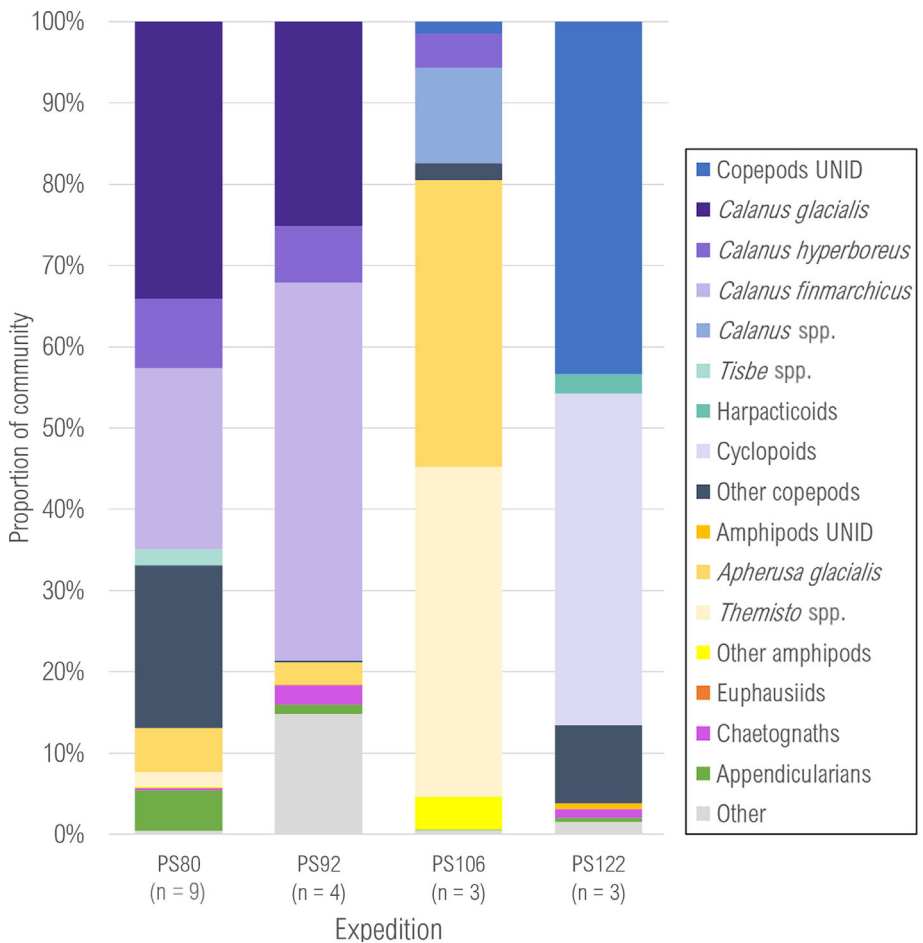


FIGURE 4 Results from the cluster analysis on diet composition of polar cod (*Boreogadus saida*) collected during four expeditions. The analysis was performed on relative diet composition data using Manhattan distance and group-average linking. Labels on the dendrogram (a) represent individual fish, which are indicated by expedition number, station number, and a reference number. Different expeditions are represented by different label colors. Taxonomic labels on the dendrogram refer to the dominating food item in the stomachs from that cluster. Red rectangles highlight groups of individuals with similar dominant species in the diet. The map (b) shows the location of the individual fish, colored according to their dominant diet item. AP, appendicularian; AT, *Apherusa/Tisbe*; CC, calanoid copepod; KR, krill.

appendicularians, and a combination of *A. glacialis* and/or *Tisbe* sp. (Figure 4a). Stations located north of Svalbard and the Fram Strait (between 20° west and 30° east), as well as station 248 (PS80) located in the Nansen basin, were dominated by calanoid copepods, whereas the other stations, located more north and east, were dominated by *A. glacialis* and/or *Tisbe* sp. (Figure 4b). There were some exceptions from this general pattern. In the former region (north of Svalbard/western Nansen basin), stomach

contents of fish collected at station 67_5 during PS106/2 were dominated by krill or *A. glacialis*. During PS80, stomach contents of all fish at station 216 and most fish at station 223 were also dominated by *A. glacialis*. In the latter region (north/east), the PS122 stations (located east of 100° east) contained few recognizable food items, with the exception of one stomach that was dominated by appendicularians and the stomach of the fish collected in winter, which was dominated by calanoid copepods.

FIGURE 5 Relative abundance of zooplankton in the ice–water interface from samples collected in the vicinity of collected fish. Samples from PS80 and PS92 were collected using a Surface and Under-Ice Trawl (SUIT). Samples from PS106/2 (referred to as PS106) and PS122 were collected using a remotely operated vehicle (ROV) net. (n) represents the number of stations from which data were used. “Other copepods” include *Metridia longa*, *Paraeuchaeta* spp., *Pseudocalanus* spp., and *Jaschnovia brevis*. For PS122, these include calanoids. The category “Other” includes ctenophores, cnidarians, polychaetes, cirripedia nauplii, foraminifera, isopods, mollusks, and ostracods.



3.3 | Available zooplankton prey under the sea ice

The under-ice mesozooplankton community sampled during PS122 consisted mainly of small copepods, cyclopoids, and small unidentified copepods (Figure 5). Due to the small mesh-size, the relative contribution of several prey items of *B. sarda* (i.e., chaetognaths, appendicularians, and amphipods) were relatively rare underneath the ice at all three sampled stations. Because the stations were sampled at very different times of the year, a detailed zooplankton community composition can be found in Figure S4.

A comparison of the relative abundances of zooplankton taxa from the ice–water interface collected during the other expeditions shows that, on average, *Calanus* spp. comprised the largest proportion of the community followed by other copepods and amphipods (Figure 5). *Calanus* spp. were present at all stations during PS80, PS92, and PS106/2 (David et al., 2015; Ehrlich et al., 2020). The proportion of the amphipods *A. glacialis* and *Themisto* spp. was relatively high at the three stations sampled during PS106/2 and species such as *A. glacialis*, *T. libellula*, and *Onisimus glacialis* were present at almost all stations during PS80 (David et al., 2015).

The calculated Ivlev's electivity indices indicated that there was positive selection for *A. glacialis* and *Tisbe* sp. ($E_i = 0.50$ and 0.92 , respectively) during PS80. The value was negative for *Calanus* spp. ($E_i = -0.59$), and close enough to zero to suggest random feeding on

Themisto spp. ($E_i = 0.18$). During PS92, the index suggested random feeding on *Calanus* spp., chaetognaths, and appendicularians ($E_i = 0.06$, 0.01 , and 0.12 , respectively) and negative selection or inaccessibility of *A. glacialis* ($E_i = -0.93$). Positive selection was indicated for *Calanus* spp. during PS106/2 ($E_i = 0.69$) and negative selection or inaccessibility for *A. glacialis* ($E_i = -0.95$). No feeding occurred on *Themisto* spp. even though they were available in the environment, whereas feeding occurred on euphausiids even though they were not found in the zooplankton community, resulting in E_i values of -1 and 1 , respectively. During PS122, positive selection was suggested for appendicularians ($E_i = 0.99$) and negative selection or inaccessibility for *Calanus* spp. ($E_i = -0.50$). Random feeding was indicated for chaetognaths and amphipods ($E_i = 0.12$ and 0.09 , respectively). No feeding occurred on harpacticoid and cyclopoid copepods ($E_i = -1$) although the latter species was relatively abundant in the collected zooplankton samples (Figure 5).

The median abundance of *Calanus* spp. from zooplankton samples associated with sampling locations of the *Calanus* spp.-dominated diet cluster (Table 5) was at least one order of magnitude higher than in the *Apherusa*/*Tisbe*-dominated and the appendicularian-dominated diet clusters, and almost twice as high as in the krill-dominated diet cluster (Table 5). Differences in the abundances of the other dominant taxa *A. glacialis*, appendicularians, and euphausiids between the four clusters were less pronounced. The ratio of *Calanus* spp. versus *A. glacialis* was

TABLE 5 Abundance of under-ice prey species ($n \text{ m}^{-2}$) and abundance ratio of *Calanus* spp. versus *Apherusa glacialis* and Appendicularia, respectively, at stations from the three major polar cod (*Boreogadus saida*) diet clusters.

Cluster	N	<i>Calanus</i> spp.	<i>A. glacialis</i>	Appendicularians	Euphausiids	Ratio <i>Calanus</i> spp. / <i>A. glacialis</i>	Ratio <i>Calanus</i> spp. / appendicularians	Ratio <i>A. glacialis</i> / appendicularians
Apherusa / Tisbe-dominated diet	8	1.6 (0.1–8.3)	0.5 (0.0–7.7)	0.0 (0.0–0.7)	0.0 (0.0–0.0)	2.0 (0.5–13.0)	23.9 (8.4–39.5)	3.6 (3.0–4.2)
Calanus spp.-dominated diet	11	15.3 (0.0–172.6)	0.7 (0.0–7.5)	0.3 (0.0–5.3)	0.0 (0.0–0.5)	13.2 (0.1–409.4)	10.1 (0.7–116.6)	1.3 (0.0–112.0)
Appendicularia-dominated diet	3	0.2 (0.0–6.2)	0.8 (0.6–2.2)	0.3 (0.0–0.7)	0.0 (0.0–0.0)	0.3 (0.1–2.8)	6.0 (0.7–8.4)	3.0 (2.4–112.0)
Krill-dominated diet	1	8.3	7.7	0.0	0.0	1.1	n.a.	n.a.

Note: Values are median values with ranges in parentheses. N = number of stations where under-ice fauna was sampled.

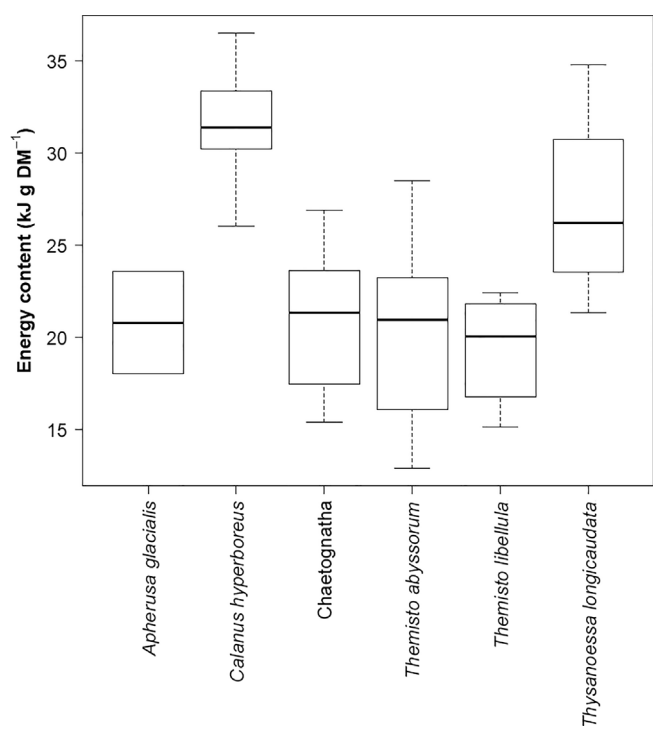


FIGURE 6 Comparison of measured mass specific energy contents of zooplankton prey of polar cod (*Boreogadus saida*).

highest in the *Calanus*-dominated diet cluster; the ratio of *Calanus* spp. versus appendicularians was lowest in the appendicularian-dominated diet cluster; and the ratio of *A. glacialis* versus appendicularians was highest in the *Apherusa/Tisbe*-dominated diet cluster (Table 5). Abundance ratios were not calculated for euphausiids because they were likely not sampled quantitatively by the ROV net.

3.4 | Energy content of zooplankton prey species

The energy content of *C. hyperboreus* was significantly higher than that of *A. glacialis*, chaetognaths, and both *Themisto* spp. (ANOVA $F_{5,61} = 33.38$, $p < 0.001$; THSD $p < 0.001$; Figure 6). On a seasonal

scale, the lowest energy content of *C. hyperboreus* was found in the water column sampled during May and July 2020 (0–200 and 0–750 m depth, respectively) and the highest in the surface waters (0–10 m) during July 2020 (Table 6). The energy content of *T. longicaudata* was significantly higher than that of both *Themisto* spp. (THSD $p \leq 0.01$).

3.5 | Predictors of growth rate

The modeled growth rates were strongly positively correlated with stomach fullness (P) (Pearson correlation: $R = 0.9$, $p < 0.001$; Figure 7a) followed by the energetic content of the ingested prey (Pearson correlation: $R = 0.49$, $p < 0.001$; Figure 7b). Temperature showed no significant correlation with growth rate (Pearson correlation: $R = -0.21$, $p = 0.078$), which is likely due to the small range of temperature values (Figure 7c). A linear model using the growth rates as response variable and all three predictors as explanatory variables indicated that stomach fullness contributed 82% and energetic content of ingested prey contributed 15% to the explained variance, whereas temperature contributed <3% (Figure 7d).

For modeled growth rates per cluster (Figure 8), indicated by its dominant prey item, highest growth rates were achieved on a diet consisting mainly of calanoid copepods and krill, although the range of growth rates when feeding mainly on calanoid copepods was quite large, and there was only one individual with a krill-dominated diet for which the growth rate could be estimated (Figure 8). Diets dominated by *Apherusa/Tisbe* or appendicularians yielded a similar range in growth rates.

4 | DISCUSSION

4.1 | Stomach content analysis of immature *B. saida* from the CAO

Given the scarcity of information of the diet of *B. saida* residing in the CAO, our study provides rare information on *B. saida*'s use of available

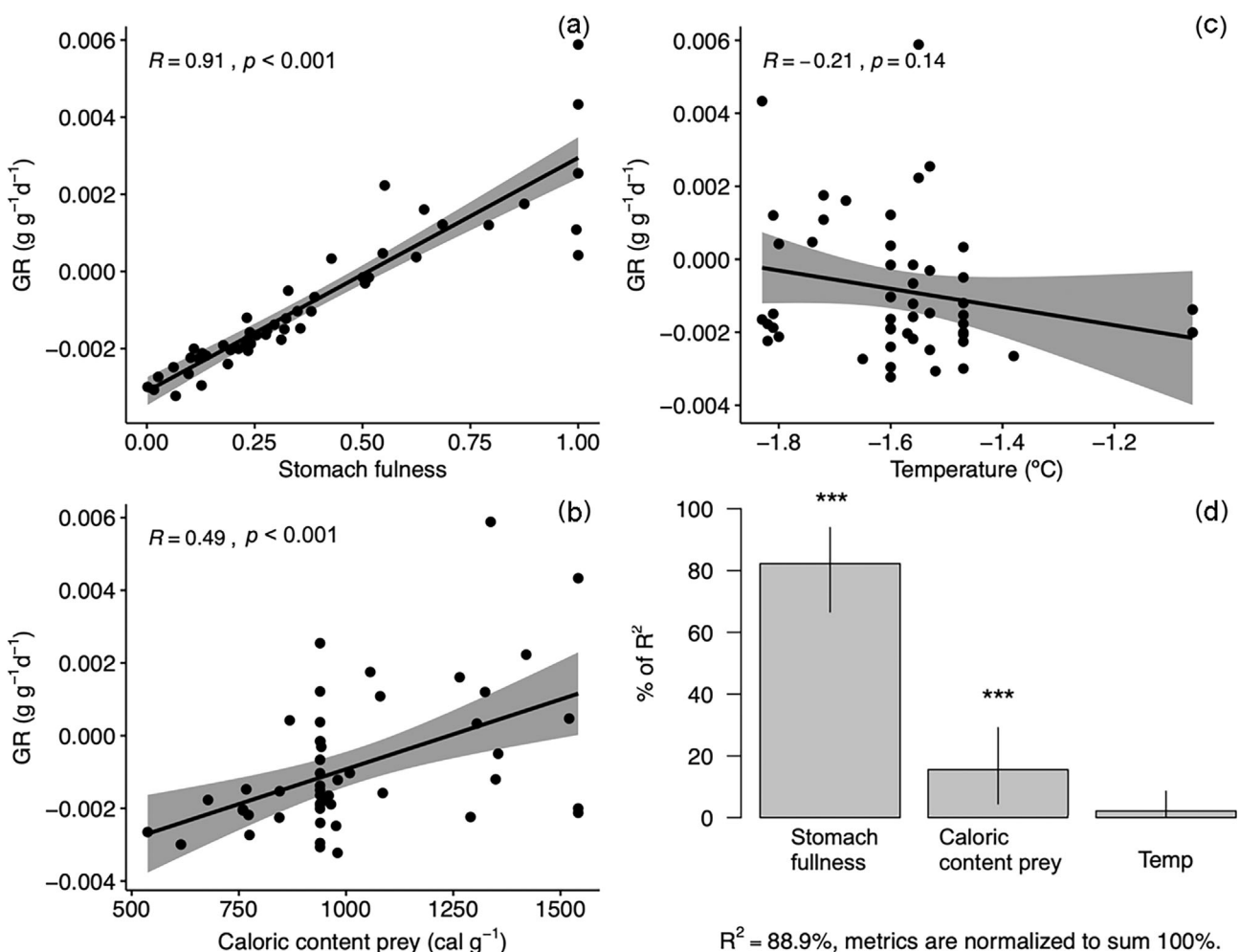
TABLE 6 Energy contents of zooplankton prey species collected during expeditions PS92 and PS122.

EXP	Species	Sampling period	Sampling depth (m)	N	n	L_T or L_P (mm) \pm SD	Energy content (kJ.g $^{-1}$ M _D) \pm SD
PS122	<i>Apherusa glacialis</i>	Jan.–April 2020	Various (1–1000)	1	5	9.1 \pm 1.7	23.6
PS122	<i>A. glacialis</i>	July 26, 2020	Surface	1	20	6.7 \pm 1.5	18.0
PS122	<i>Calanus hyperboreus</i>	Nov. 14, 2019	0–200	4	20	6.7 \pm 0.3	30.9 \pm 1.5
PS122	<i>Calanus hyperboreus</i>	Jan. 7, 2020	0–200	3	30	6.6 \pm 0.3	30.6 \pm 1.5
PS122	<i>C. hyperboreus</i>	Jan. 8, 2020	200–2000	2	20	6.5 \pm 0.4	33.8 \pm 0.1
PS122	<i>C. hyperboreus</i>	Jan. 22, 2020	0–200	3	30	6.6 \pm 0.3	32.0 \pm 1.2
PS122	<i>C. hyperboreus</i>	Jan. 29, 2020	200–2000	3	30	6.3 \pm 0.5	31.4 \pm 2.5
PS122	<i>C. hyperboreus</i>	May 6, 2020	0–200	3	24	6.6 \pm 0.3	31.13 \pm 0.3
PS122	<i>C. hyperboreus</i>	May 7, 2020	0–200	2	17	6.5 \pm 0.3	28.7 \pm 3.7
PS122	<i>C. hyperboreus</i>	July 8, 2020	0–750	3	30	6.6 \pm 0.2	29.1 \pm 2.2
PS122	<i>C. hyperboreus</i>	July 19, 2020	0–10	3	30	6.6 \pm 0.3	35.6 \pm 0.8
PS122	<i>C. hyperboreus</i>	Sept. 12, 2020	0–100	4	29	6.6 \pm 0.4	32.8 \pm 14.8
PS122	Chaetognatha	Dec. 28, 2019	0–1000	1	1	NA	17.5
PS122	Chaetognatha	Nov. 2019–Jan. 2020	Various (1–1000)	1	9	NA	23.4
PS122	Chaetognatha	Jan.–July 2020	Various (95–2000)	1	8	NA	20.3
PS122	Chaetognatha	Dec. 28, 2019	0–1000	1	6	NA	15.6
PS122	Chaetognatha	Jan. 14, 2020	200–2000	1	6	NA	25.3
PS122	Chaetognatha	Jan. 14, 2020	200–2000	1	6	NA	21.4
PS122	Chaetognatha	April 25, 2020	95	1	5	NA	15.4
PS122	Chaetognatha	June 16, 2020	0–200	1	9	NA	23.6
PS122	Chaetognatha	June–July 2020	0–200	1	8	NA	26.9
PS92	<i>Themisto abyssorum</i>	June 9, 2015	200–500	2	10	13.2 \pm 1.9	20.9 \pm 0.2
PS92	<i>T. abyssorum</i>	June 9, 2015	200–500	3	3	11.0 \pm 1.4	16.8 \pm 3.6
PS122	<i>T. abyssorum</i>	July 8, 2020	0–750	1	5	9.6 \pm 1.3	20.4
PS122	<i>T. abyssorum</i>	Sept., 17 2020	0–1000	7	7	11.9 \pm 0.8	21.7 \pm 5.3
PS122	<i>T. abyssorum</i>	Sept. 17, 2020	0–1000	1	6	10.2 \pm 1.0	12.9
PS92	<i>T. libellula</i>	June 17, 2015	0–2	3	14	19.9 \pm 1.9	16.8 \pm 2.3
PS92	<i>T. libellula</i>	June 21, 2015	0–2	5	5	31.6 \pm 3.1	20.9 \pm 1.9
PS122	<i>Thysanoessa longicaudata</i>	Jan. 7, 2020	0–200	1	3	15.0 \pm 1.0	26.7
PS122	<i>T. longicaudata</i>	July 8, 2020	0–750	1	8	12.4 \pm 1.8	21.4
PS122	<i>T. longicaudata</i>	Nov. 15, 2019	0–1000	1	6	15.2 \pm 1.3	25.7
PS122	<i>T. longicaudata</i>	June 16, 2020	0–200	1	9	11.3 \pm 2.5	34.8

Abbreviations: EXP, expedition number; L_P , prosome length, which was measured for the copepod *Calanus hyperboreus*; L_T , total length, which was measured for the amphipod and euphausiid species; N, number of caloric content measurements performed; n, total number of individuals used.

prey and of the sea ice, at various habitats in a difficult-to-investigate region. The stomach contents of *B. saida* from the sea-ice habitat of the CAO showed that the diet was variable. Dominant prey items included predominantly sympagic species such as *A. glacialis* and *Tisbe* sp., and pelagic species such as *Calanus* spp., appendicularians, chaetognaths, and krill. In the few previous studies available, copepods and amphipods were the most prominent prey items in the stomachs of fish collected from underneath the sea ice located north of Svalbard (Lønne & Gulliksen, 1989; Renaud et al., 2012) or in the CAO (Andriashev et al., 1980). Lønne and Gulliksen (1989) sampled

26 *B. saida* in the multiyear ice north of Svalbard and reported calanoid copepods and the amphipods *A. glacialis* and *Themisto libellula* as the main prey items in terms of occurrence, numbers, and biomass. Chaetognaths and appendicularians were found in their diet assessment but in relatively low numbers, whereas the results of our study suggest that these can be important prey items for *B. saida*. Lønne and Gulliksen (1989) also found relatively large proportions of other sympagic amphipods, ostracods, and gastropods in the stomachs of the fish, which were not observed in the stomachs of the fish in our study. Renaud et al. (2012) found mainly *Themisto* spp. and *A. glacialis*



$R^2 = 88.9\%$, metrics are normalized to sum 100%.

FIGURE 7 Effects of stomach fullness, energetic content of prey, and water temperature on growth rates (GR). Pearson correlation (black lines) between GR and (a) stomach fullness, (b) energetic content g⁻¹ ingested prey and (c) temperature. The regression coefficients and statistical significances are given for each predictor. (d) Relative contribution of each predictor to GR (% of R^2), evaluated with a linear regression model ($p < 0.001$ ***).

in the stomachs of 21 fish collected from within sea-ice crevices at a single location in September. The specimens collected in the studies of Lønne and Gulliksen (1989) and Renaud et al. (2012) were of sizes similar to the fish collected during our study. Size may influence diet composition, as larger fish tend to consume larger prey (Matley et al., 2013; McNicholl et al., 2016; Renaud et al., 2012).

In our study, several ways to express diet composition were used to assess the importance of prey species in the diet of *B. saida* (Buckland et al., 2017; Hyslop, 1980), such as reconstructed dry mass, the frequency of occurrence, and the calculated index of relative importance, to minimize the bias that may occur due to differences in digestibility of the prey consumed (Buckland et al., 2017). For example, small organisms may be digested more rapidly than larger ones (Sutela & Huusko, 2000), and soft-bodied zooplankton species are digested more rapidly than hard-bodied species (Sikora et al., 1972). Such differences may influence the recognizability, and thus the relative abundance, of certain prey items in the stomach contents. Although microscopic stomach content analysis provides crucial

information to understand feeding dynamics of *B. saida*, enabling the linkage between available and ingested food, it only shows a snapshot of the diet and likely underestimates prey diversity (Maes et al., 2022). Complementing this method with other methods, such as DNA metabarcoding or fatty acid analyses, may provide a more complete view of the diet of a species and information on feeding habits over longer time scales (Kohlbach et al., 2017; Maes et al., 2022; Schmidt et al., 2006). Nevertheless, our study provides further insights in the variability in immature *B. saida*'s diet and feeding behavior.

4.2 | Seasonal and regional variation in *B. Said*a diet and prey presence

Some seasonal and/or regional grouping of individuals with a similar diet composition was shown with the cluster analysis. *B. saida* with stomach contents dominated by *A. glacialis* and *Tisbe* sp. were mainly collected in the northeastern part of the sampling area during late

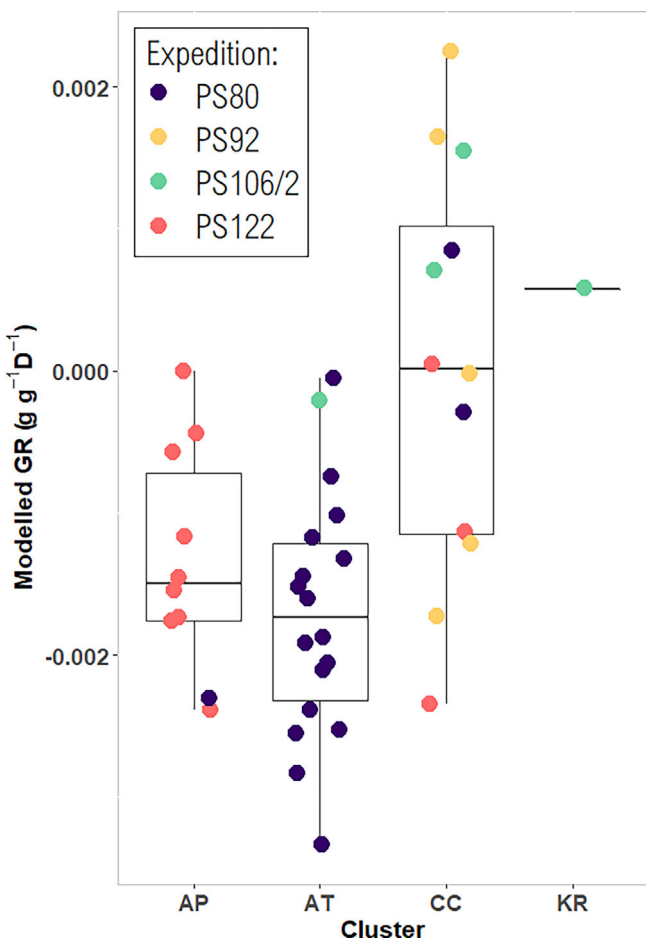


FIGURE 8 Modeled growth rates (GR) per diet type (cluster, based on Figure 4). In the boxplots, the horizontal black lines show the median GR in a cluster. The upper and lower limits of the colored squares indicate the 25th and 75th percentiles, respectively. The upper and lower limits of the vertical line indicate the minimum and maximum GR, respectively, in a cluster. AP, appendicularian dominated; AT, *Apherusa glacialis* and *Tisbe* sp. dominated; CC, calanoid copepod dominated; KR, krill dominated. Overlying points represent the modeled growth rate for each individual fish, colored based on the expedition during which they were sampled.

summer/autumn in the inner CAO, whereas samples with a *Calanus*-dominated diet were mainly taken in the Atlantic Gateway region north of Svalbard during spring/early summer. Differences in the diet may be explained by regional and/or seasonal differences in prey presence, which may depend on environmental properties, including those of the sea ice (David et al., 2015; Ehrlich et al., 2020, 2021; Flores et al., 2019; Lønne & Gulliksen, 1991). Seasonal patterns in density and distribution of zooplankton in the upper water column have been found for several prey species. Mature individuals of *A. glacialis* are usually not as abundant in the ice–water interface during spring compared to summer (Ehrlich et al., 2020; Melnikov & Kulikov, 1980 in Gulliksen & Lønne, 1989), and abundances have been suggested to be positively related to melting conditions (Werner & Gradinger, 2002). The absolute densities as found during our spring expeditions were, however, similar or higher compared to those from

the summer/autumn expedition (PS80), although the use of a different gear in the spring expedition during which highest *A. glacialis* abundances were found (PS106/2) might compromise comparability (David et al., 2015; Ehrlich et al., 2020). The numbers or availability of *Tisbe* spp. may increase in the water column when the sea ice starts to melt and in-ice copepods move from the sea ice into the water below (Grainger et al., 1986). This may be why *Tisbe* sp. or harpacticoid copepods only occurred in net samples collected during the summer (David et al., 2015; fig. 5). *C. glacialis* has been found accumulating closer to the sea-ice underside during spring (April/May) and feeding on the ice-algal bloom occurring during this time (Runge & Ingram, 1988). Although *Calanus* spp. were the dominant species in the zooplankton communities from both summer/autumn (PS80) and spring (PS92), the absolute densities of all three *Calanus* spp. were an order of magnitude higher during spring compared to summer/autumn (David et al., 2015; Ehrlich et al., 2020).

It remains difficult to disentangle seasonal from regional effects, as the expeditions covered different regions in different seasons. Bottom topography, water mass properties, and circulation patterns result in different environmental properties among and within regions, which are known to affect the zooplankton community structure (David et al., 2015; Ehrlich et al., 2020). For example, the environments of the Nansen and Amundsen basins have been found to differ in terms of, for example, sea-ice thickness, salinity, mixed-layer depth, surface chlorophyll *a* concentrations, and nutrients, which were reflected in the zooplankton community structure (David et al., 2015; Flores et al., 2019). Differences in environmental conditions affected some species more than others. *C. hyperboreus*, *C. glacialis*, and *Onisimus nansenii* were present in different densities depending on the sampled basin, whereas species such as *A. glacialis* and *O. glacialis* were present more uniformly throughout the survey area (David et al., 2015). Another example can be found in the area north of Svalbard, where environmental conditions over the Yermak Plateau differed from those in the adjacent basin, which also affected the zooplankton community structure (Ehrlich et al., 2020).

Apart from the relatively small sample size of *B. sarda* during several years in this study, natural annual variability in prey density and distribution may hamper the discovery of a clear temporal or spatial pattern in the diet of *B. sarda*, as the biomass of the sympagic community can vary greatly from year to year (Lønne & Gulliksen, 1991). Fish size could be another aspect influencing diet variability, as the individuals collected during PS80 were statistically smaller than the fish collected during the other expeditions. The size overlap between PS80 fish and fish from the other expeditions, as well as the size ranges of the ingested prey and seasonal/regional differences among relative abundances of prey present in the environment, suggests, however, that fish size is not the major explanatory factor of diet variability.

4.3 Feeding behavior and prey presence

Our results generally agree with previous studies indicating that *B. saída* can be considered an opportunistic feeder (Craig et al., 1982;

Gray et al., 2016; Lønne & Gulliksen, 1989; Majewski et al., 2016), with differences in diet likely resulting from relative differences in the availability of different prey types (Figure 4; Table 5). However, *B. saida* appeared to not always feed on the dominant prey species present as apparent from net-based zooplankton sampling, calculated electivity indices, and abundance ratios of prey. For example, during late summer/autumn (PS80), when *B. saida* were found feeding mainly on *A. glacialis* and *Tisbe* sp., the more energy-rich *Calanus* spp. were also available in quantities that exceeded those of both *A. glacialis* and *Tisbe* sp. (David et al., 2015; Ehrlich, 2015; Figure 5; Table 5). Although the mesh size used during sampling may have been too large for catching *Tisbe* sp. quantitatively, and their densities in the ice-water interface were likely underestimated, the number of *Calanus* spp. in the ice-water interface exceeded those of *Tisbe* sp. up to 50 times (David et al., 2015). Individuals of *A. glacialis* are usually larger than *Calanus* spp., likely resulting in a better trade-off between energy invested per captured prey individual and energy intake from feeding. In contrast, *Tisbe* sp. are much smaller than *Calanus* spp., implying that a different energetic trade-off mechanism explains their high numerical abundance in the diet composition during PS80. We hypothesize that *Tisbe* spp. were energetically more efficient to capture than *Calanus* spp. in areas where *Tisbe* sp. were abundant, possibly due to dense aggregation in sea-ice crevices, and due to a lower escape range because of their small size. Due to their association with sea ice, and imaginably accumulation in crevices, both *A. glacialis* and *Tisbe* sp. can be caught in the shelter of the ice (David et al., 2015; Werner & Martinez-Arbizu, 1999), possibly further reducing the *B. saida*'s energy expenditure on swimming and hunting. In addition, the accumulation at the sea ice may not only increase their concentration but also reduce their routes for escape by itself, increasing prey encounter rates and prey capture efficiency. Comparing the median relative abundance of *Calanus* spp. versus *A. glacialis*, however, the ratio was almost one order of magnitude lower at the stations where *Apherusa/Tisbe*-dominated the *B. saida* diet than at stations where *Calanus* spp. dominated the diet. This indicates that, below a certain abundance threshold, the effort to capture *Calanus* spp. was greater than the energetic gain (Table 5). The results of our study suggest that *B. saida* use a feeding strategy that minimizes energy expenditure for moving, prey capture, and digestion, favoring prey that occur in high densities and/or are easy to catch. Thus, feeding does not solely depend on prey presence but on a combination of prey density and catchability, and possibly digestibility. Results also show that positive or negative selection for certain prey does not only depend on the density of that species but also on the densities of other prey species present in the area. Abundance thresholds at which prey become energetically more favorable may change with fish size as, for example, catchability of certain prey species may increase with increasing size.

The stomach contents of the *B. saida* collected during PS122 were mainly appendicularian-dominated. This could indicate that the young *B. saida* actively select for appendicularians as suggested by E_i , and may, therefore, co-occur in the area. It may also indicate that the stomach contents of the fish investigated were not entirely

representative of an average diet composition of fish in that region or during that time. Data on prey distribution suggest that appendicularians were not omnipresent in the area during sampling. Very high abundances of appendicularians were found at several locations in studies of the ice-water interface, suggesting a highly patchy distribution (David et al., 2015; Ehrlich et al., 2020). In addition, the majority of the fish were collected in a single small-scale sampling event during PS122. Nevertheless, these findings do substantiate results, also derived from the growth rate model, that *B. saida* tend to utilize dense patches of prey even if less optimal in terms of energetic value such as suggested for appendicularians. Nakano et al. (2016) found *B. saida* feeding on appendicularians (47% and 50% I_{RI} , respectively) in the northern Bering Sea and southern Chukchi Sea despite high abundances of copepods in the areas. The researchers suggested that their very large houses, observed by ROV, slow swimming speed, and lack of carapace make them easy to catch and digest (Nakano et al., 2016). Although no evidence of ingestion was seen in *B. saida*'s stomach contents, previous studies did report ingestion, and even active selection, of secreted appendicularian houses, which have been thought to be an underestimated source of carbon (summarized in Jaspers et al., 2023).

The zooplankton community was not collected simultaneously with the fish during PS106/2 and PS122 as data were derived from the ROV net. This is in contrast to PS80 and PS92, when fish and their prey were sampled at the same time using the SUIT. Results from PS106/2 indicate that zooplankton analysed from samples collected at stations near where fish were caught (in both space and time) may not always provide an accurate local representation of available prey. During this expedition, only a few specimens ($n = 5$) of *B. saida* were collected at a few stations ($n = 3$), but the variation in diet composition was large (Figure 4). Therefore, the *B. saida* from this expedition were grouped into several clusters, including a cluster containing fish with a krill-dominated diet. Euphausiids are not particularly known to reside in surface waters, but elevated densities of *T. longicaudata* and *Thysanoessa inermis* occurred at the ice-water interface during PS106/2 (H.F., personal communication; Schaafsma et al., 2022), explaining their presence in the *B. saida* stomachs during this expedition. The ROV net is too small to collect euphausiids, in contrast to the SUIT. Although the amphipods *A. glacialis* and *T. libellula* were, on average, abundant in the ice-water interface during PS106/2, relative numbers of amphipods and *Calanus* spp. also varied greatly in zooplankton samples collected during this expedition.

4.4 | Modeled *B. saida* growth rate

The bioenergetic model provides insights in the sensitivity of *B. saida* growth to variation in prey fields. It shows that growth rate may be more sensitive to the amount of food ingested, defined in the model through stomach fullness and, to a lesser degree, the energetic content of prey. This is primarily explained by the data distribution of the two parameters in the model having different coefficients of variation, that is, ratio between SD and the mean. Nonetheless, the high

importance of stomach fullness in the model could indicate that the benefit of high-energy prey may be counterbalanced by other factors, such as energy expenditure for prey capture or minimizing predation risk. Such findings agree with our microscopic analysis indicating preferred feeding on prey that is abundant and/or easily available and/or prey that can be collected with relatively low effort. Although highest growth rates were found when *B. sarda* fed predominantly on energy-rich prey, such as *Calanus* spp. or krill (Figure 8), our comparison of prey composition with the abundances of various key prey taxa indicates that the energetic trade-off for such high-energy prey depends strongly on its abundance and the abundance of alternative prey (Figure 5; Table 5).

The effect of subzero temperatures on metabolic rates at sampling could explain the low modeled growth rates. Near-zero temperatures have been experimentally shown to induce low stomach evacuation rates and high assimilation rates in *B. sarda* (Hop & Tonn, 1998), resulting in enhanced feed conversion efficiency at low feed intake (Kunz et al., 2016). This could explain the good body condition of *B. sarda* caught at subzero temperature, while the model indicated low growth rates, suggesting model constraints in its temperature-limitation functions. Unfortunately, we lack crucial data from subzero temperatures to correctly model *B. sarda* adaptation to ice habitat.

Results from model simulations should be interpreted while considering the simplifications and specific assumptions that have been made (David et al., 2022), including a fixed ratio between active and basal metabolic rates and a constant energetic content of fish and prey types. An averaged energetic content per prey species was used for all sampled fish, although several prey species are known to have varying energy contents over the course of the year or with size (e.g., Kraft et al., 2015; Nowicki et al., 2023; Percy & Fife, 1981). This could reduce the variability in modeled growth rates. However, seasonal variation in the energy content of a species is likely much less than the variation between species.

Although it is not surprising that both stomach fullness and prey energy content influence growth rate, the results indicate that changes in the abundance and catchability of the prey, and thus the amount of prey ingested, may have a larger impact than changes in prey energy content. With the warming of the Arctic Ocean and a shift toward smaller copepods and higher abundances of gelatinous zooplankton species, a number of prey field characteristics will change for *B. sarda* such as the density, the size spectrum, the energy content, and the catchability of prey. The latter is due to potential changes in the density and behavior of the prey, as well as the loss of the under-ice habitat as a major feeding ground. Changes in such characteristics should thus be taken into account when anticipating consequences of environmental changes for *B. sarda*.

4.5 | Energy content of *B. sarda* prey species

Energy content measurements on most species from our study generally corresponded well with findings from the literature

(Båmstedt, 1981; Norrbin & Båmstedt, 1984; Nowicki et al., 2023; Percy & Fife, 1981). Variations in energy content with season and body size have been found for various species. The energy content of the krill species *T. inermis* did not vary between winter and summer, but larger specimens had a higher energy content than smaller ones (Nowicki et al., 2023). For another krill species, *Meganyctiphanes norvegica*, variation between summer and winter was found, with values of 22.71 and 24.60 kJ g⁻¹ M_D, respectively (Nowicki et al., 2023). Energy contents decreased in winter (18.77 and 17.83 kJ g⁻¹ M_D) compared to summer (23.07 and 21.13 kJ g⁻¹ M_D) for both *T. libellula* and *T. abyssorum*, respectively (Nowicki et al., 2023). Individuals of *T. libellula* larger than 30 mm were found to have a higher energy content compared to smaller individuals, but for individuals <20 mm, there was no difference between size classes of *T. libellula* nor was there a difference with similar-sized *T. abyssorum* (Nowicki et al., 2023). This suggests that the energy content measurements we performed on *T. libellula* and *T. abyssorum* can be regarded as representative for the individuals ingested by the *B. sarda* in our study.

In the growth rate model, the energy content of *Calanus* prey was based on measurements performed on *C. hyperboreus*. Size measurements performed on *Calanus* spp. from the stomachs suggest, however, that the stomach contents likely contained a majority of *C. finmarchicus* and/or *C. glacialis*. The energy contents of the three *Calanus* species may vary, largely because lipid contents depend on developmental stage, season, and region due to the different life cycles and distribution patterns of the three *Calanus* species (e.g., Graeve et al., 2005; Kattner et al., 1989; Kirkesæter, 1978 in Båmstedt, 1981; Scott et al., 2000; Swalethorpe et al., 2011). Although some studies indicate that the energy density or lipid content per weight unit can be similar among the three species (Davies et al., 2012; Kohlbach et al., 2016), the smaller sizes indicate that energy content per individual would be less for *C. glacialis* and *C. finmarchicus* compared to *C. hyperboreus*.

5 | CONCLUSIONS

Results of our study suggest that *B. sarda* are flexible in their feeding modes, capable of utilizing a diverse range of both sympagic and pelagic resources. Consequences of climate warming for their growth and survival will depend not only on prey presence alone but also on prey catchability, digestibility, and energy content. Climate models predict that the Arctic could be completely ice-free in summer as early as 2030 (Guarino et al., 2020; Kim et al., 2023). This shows that the window of opportunity to sample the sea ice-associated high Arctic food web in summer is rapidly closing. In this context, the compiled information on the stomach content of 85 immature *B. sarda* sampled directly under sea ice in the CAO represents a rare baseline for future studies. A change in Arctic zooplankton community composition and vertical distribution, and thus in available prey, is expected as a consequence of climate warming and concomitant sea-ice loss (e.g., Flores et al., 2023;

Kvile et al., 2018; Møller & Nielsen, 2020; Polyakov et al., 2020; Tittensor et al., 2021). It remains difficult to predict consequences of climate change on the growth and survival of *B. saida* in the CAO, which requires further data on the variation of its diet, a better understanding of zooplankton distribution in relation to environmental parameters, and an understanding of how food requirements depend on temperature. However, the possible impact of changes in the zooplankton community composition affecting the amount of food that *B. saida* can capture and eat in an energy-efficient way may have been underestimated in the past compared to changes in the energetic contents of the available prey.

AUTHOR CONTRIBUTIONS

Conceptualization and study design: Hauke Flores and Fokje L. Schaafsma. Study design MOSAiC: Hauke Flores, Fokje L. Schaafsma, Barbara Niehoff, and Pauline Snoeijis-Leijonmalm. Fieldwork: Fokje L. Schaafsma, Hauke Flores, Carmen L. David, Giulia Castellani, Serdar Sakinan, André Meijboom, Barbara Niehoff, Nicole Hildebrandt, Katrin Schmidt, Pauline Snoeijis-Leijonmalm, Julia Ehrlich, Carin J. Ashjian, and MOSAiC team ECO. Stomach content analysis: Fokje L. Schaafsma and Hauke Flores. Energy content analysis: André Meijboom and Fokje L. Schaafsma. Environmental data preparation: Giulia Castellani. Growth rate analysis and figure preparation: Carmen L. David. PS122 ROV net sample analysis: Astrid Cornils. All other statistical analyses and figures: Fokje L. Schaafsma. Main text: Fokje L. Schaafsma, Hauke Flores, and Carmen L. David. All authors contributed to the writing of the manuscript and approved the submitted version to be published.

ACKNOWLEDGMENTS

We thank all those who contributed to MOSAiC and made this endeavor possible (Nixdorf et al., 2021). Thanks to the additional members of team ECO for their help with sample collection, organization, and coordination, and to Martina Vortkamp, Lena Eggers, and Anja Nicolaus for MOSAiC sample logistics. We are very grateful to the captains and crew of R.V. *Polarstern* for their support with the work at sea. We thank Michiel van Dorssen for technical support using SUIT during expeditions PS80 (IceArc), PS92 (TRANSSIZ), and PS106/2 (SIPES). We thank Benjamin Lange (PS80 and PS106/2), Martina Vortkamp (PS92), Antonia Immerz (PS92), Sarah Zwicker (PS92), Erik Sulanke (PS106/2), Kim Vane (PS106/2), Elisa Bravo Rebolledo (PS106/2), Nils Koschnick (PS106/2), Jennifer Steffen (PS106/2), and Erin Kunisch (PS106/2) for their help with the sampling of fish and zooplankton. Mai Apasiri Klasmeier helped with the stomach content analysis of polar cod collected during PS106/2, and Nadya Zakharova helped with the analysis of zooplankton samples from PS106/2. We also thank Benjamin Lange for help with environmental data collection and preparation, Marinka van Puijenbroek for help with preparing the map (Figure 1), and Thomas Krumpen for providing MOSAiC sea-ice concentration. PS122 data used in this manuscript were produced as part of the international Multidisciplinary drifting

Observatory for the Study of the Arctic Climate (MOSAiC) with the tag MOSAiC20192020.

FUNDING INFORMATION

Work during the MOSAiC expedition was funded by the Dutch Research Council grant 866.18.003, with contributions of the European Commission (EC), European Climate, Infrastructure and Environment Executive Agency (CINEA), Framework Contract EASME/EMFF/2018/003, Specific Contract EASME/EMFF/2018/1.3.2.2/03/SI2.805469, and of the Netherlands Ministry of Agriculture, Nature and Food Quality (LNV) grant WOT-04-009-047.04. The work during the other expeditions was supported by Dutch Research Council grant 866.13.009, the Helmholtz Association through the Young Investigators Group *Iceflux* (VH-NG-800) and the Netherlands Ministry of LNV. Hauke Flores and Barbara Niehoff were funded by the Helmholtz Association's Programme Oriented Funding Period 4 (POF-4), work packages 6.1 and 6.3. Astrid Cornils was funded by the Bundesministerium für Bildung und Forschung (BMBF) (grant 03F0917A MOSAiC 3). Katrin Schmidt was funded by the UK Natural Environment Research Council (NERC) (grant NE/S002502/1). Julia Ehrlich was funded by the national scholarships “Promotionsstipendium nach dem Hamburger Nachwuchsfördergesetz (HmbNFG)” and “Gleichstellungs fond 2017 (4-GLF-2017),” both granted by the University of Hamburg. Expedition grant numbers: ARK XVII/3 (PS80; IceArc), AWI_PS92_00 (TRANSSIZ), AWI_PS106/1_2-00 (SIPCA), and AWI_PS122_00 (MOSAiC).

CONFLICT OF INTEREST STATEMENT

The authors declare that the research was conducted in the absence of any commercial or financial relationships that could be construed as a potential conflict of interest.

DATA AVAILABILITY STATEMENT

The following datasets were generated: Diet of polar cod (*Boreogadus saida*) from the central Arctic Ocean (Schaafsma et al., 2024. PANGAEA, <https://doi.pangaea.de/10.1594/PANGAEA.956722>). Energy content measurements on Arctic zooplankton collected during MOSAiC (PS122) (Schaafsma et al., 2023. PANGAEA, <https://doi.org/10.1594/PANGAEA.954789>).

ORCID

Fokje L. Schaafsma  <https://orcid.org/0000-0002-8945-2868>

REFERENCES

Aguirre, G. E., Capitanio, F. L., Viñas, M. D., & Esnal, G. B. (2006). Gonadal development, allometric growth and ecological impact of *Appendicularia sicula* (Appendicularia: Fritillariidae) from the south-western Atlantic Ocean. *Journal of the Marine Biological Association of the UK*, 86, 1215–1220.

Alfred-Wegener-Institut Helmholtz-Zentrum für Polar- und Meeresforschung. (2017). Polar research and supply vessel POLARSTERN operated by the Alfred-Wegener-institute. *Journal of Large-Scale Research Facilities*, 3, A119.

Andriashov, A. P., Mukhomediyarov, B. F., & Pavshiks, E. A. (1980). On mass congregations of the cryopelagic cod fishes (*Boreogadus saida*

and *Arctogadus glacialis*) in circumpolar Arctic basins. In M. E. Vinogradov & I. A. Melnikov (Eds.), *Biology of the Central Arctic Basin* (pp. 196–211). Shirshov Institute of Oceanology, Academy of Sciences of the USSR, Nauka (Science) Press, Moscow.

Bämstedt, U. (1981). Water and organic content of boreal macrozooplankton and their significance for the energy content. *Sarsia*, 66(1), 59–66.

Bämstedt, U. (1986). Chemical composition and energy content. In E. D. S. Corner & S. C. M. O'Hara (Eds.), *The biological chemistry of marine copepods* (pp. 1–58). Clarendon Press.

Benoit, D., Simard, Y., & Fortier, L. (2014). Pre-winter distribution and habitat characteristics of polar cod (*Boreogadus saida*) in southeastern Beaufort Sea. *Polar Biology*, 37, 149–163. <https://doi.org/10.1007/s00300-013-1419-0>

Brett, J. R. (1979). 10 – environmental factors and growth. In W. S. Hoar, D. J. Randall, & J. R. Brett (Eds.), *Feish physiology* (Vol. 8, pp. 599–675). DOI). Academic Press. [https://doi.org/10.1016/S1546-5098\(08\)60033-3](https://doi.org/10.1016/S1546-5098(08)60033-3)

Buckland, A., Baker, R., Loneragan, N., & Sheaves, M. (2017). Standardising fish stomach content analysis: The importance of prey condition. *Fisheries Research*, 196, 126–140.

Castellani, G., Schaafsma, F. L., Arndt, S., Lange, B. A., Peeken, I., Ehrlich, J., David, C., Ricker, R., Krumpen, T., & Hendricks, S. (2020). Large-scale variability of physical and biological sea-ice properties in polar oceans. *Frontiers in Marine Science*, 7, 536.

Clarke, K. R., & Warwick, R. M. (2001). *Change in marine communities: An approach to statistical analysis and interpretation*. PRIMER-E Limited.

Cornils, A., Thomisch, K., Hase, J., Hildebrandt, N., Auel, H., & Niehoff, B. (2022). Testing the usefulness of optical data for zooplankton long-term monitoring: Taxonomic composition, abundance, biomass, and size spectra from ZooScan image analysis. *Limnology and Oceanography: Methods*, 20(7), 428–450. <https://doi.org/10.1002/lom3.10495>

Craig, P., Griffiths, W., Haldorson, L., & McElberry, H. (1982). Ecological studies of Arctic cod (*Boreogadus saida*) in Beaufort Sea coastal waters, Alaska. *Canadian Journal of Fisheries and Aquatic Sciences*, 39, 395–406.

David, C., Lange, B., Krumpen, T., Schaafsma, F., van Franeker, J. A., & Flores, H. (2016). Under-ice distribution of polar cod *Boreogadus saida* in the central Arctic Ocean and their association with sea-ice habitat properties. *Polar Biology*, 39(6), 981–994.

David, C., Lange, B., Rabe, B., & Flores, H. (2015). Community structure of under-ice fauna in the Eurasian central Arctic Ocean in relation to environmental properties of sea-ice habitats. *Marine Ecology Progress Series*, 522, 15–32. <https://doi.org/10.3354/meps11156>

David, C. L., Ji, R., Bouchard, C., Hop, H., & Hutchings, J. A. (2022). The interactive effects of temperature and food consumption on growth of larval Arctic cod (*Boreogadus saida*): A bioenergetic model. *Elementa: Science of the Anthropocene*, 10, 1. <https://doi.org/10.1525/elementa.2021.00045>

Davies, K. T. A., Ryan, A., & Taggart, C. T. (2012). Measured and inferred gross energy content in diapausing *Calanus* spp. in a Scotian shelf basin. *Journal of Plankton Research*, 34, 614–625.

Deudero, S., & Morales-Nin, B. (2001). Prey selectivity in planktivorous juvenile fishes associated with floating objects in the western Mediterranean. *Aquaculture Research*, 32, 481–490.

Ehrlich, J. (2015). *Diversity and distribution of high-Arctic zooplankton in the Eurasian Basin in late summer 2012*. Master Thesis. University of Hamburg.

Ehrlich, J., Bluhm, B. A., Peeken, I., Masicotte, P., Schaafsma, F. L., Castellani, G., Brandt, A., & Flores, H. (2021). Sea-ice associated carbon flux in Arctic spring. *Elementa: Science of the Anthropocene*, 9, 1. <https://doi.org/10.1525/elementa.2020.00169>

Ehrlich, J., Schaafsma, F. L., Bluhm, B. A., Peeken, I., Castellani, G., Brandt, A., & Flores, H. (2020). Sympagic fauna in and under Arctic pack ice in the annual sea-ice system of the new Arctic. *Frontiers in marine. Science*, 7(452), 1–19. <https://doi.org/10.3389/fmars.2020.00452>

Fiksen, Ø., & MacKenzie, B. R. (2002). Process-based models of feeding and prey selection in larval fish. *Marine Ecology Progress Series*, 243, 151–164. <https://doi.org/10.3354/meps243151>

Flores, H., David, C., Ehrlich, J., Hardge, K., Kohlbach, D., Lange, B. A., Niehoff, B., Nöthig, E. M., Peeken, I., & Metfries, K. (2019). Sea-ice properties and nutrient concentration as drivers of the taxonomic and trophic structure of high-Arctic protist and metazoan communities. *Polar Biology*, 42, 1377–1395. <https://doi.org/10.1007/s00300-019-02526-z>

Flores, H., Ehrlich, E., Lange, B., Sulanke, E., Niehoff, B., Hildebrandt, N., Doble, M., Schaafsma, F. L., Meijboom, A., Fey, B., Kühn, S., Bravo-Rebolledo, E., Van Dorssen, M., Gradinger, R., Hassett, B., Kunisch, E., Kohlbach, D., Graeve, M., Van Franeker, J. A., & Bluhm, B. (2018). Under-ice fauna, zooplankton and endotherms. In: The expeditions PS106/1 and 2 of the research vessel Polarstern to the Arctic Ocean in 2017, Macke a & Flores H, eds. *Berichte Zur Polar- Und Meeresforschung*, 719, 123–133. https://doi.org/10.2312/BzPM_0719_2018

Flores, H., Veyssiére, G., Castellani, G., Wilkinson, J., Hoppmann, M., Karcher, M., Valcic, L., Cornils, A., Geoffroy, M., Nicolaus, M., Niehoff, B., Priou, P., Schmidt, K., & Stroeve, J. (2023). Sea-ice decline could keep zooplankton deeper for longer. *Nature Climate Change*, 13, 1122–1130. <https://doi.org/10.1038/s41558-023-01779-1>

Gallili, T. (2015). Dendextend: An R package for visualizing, adjusting, and comparing trees of hierarchical clustering. *Bioinformatics*, 31, 3718–3720. <https://doi.org/10.1093/bioinformatics/btv428>

Geoffroy, M., Bouchard, C., Flores, H., Robert, D., Gjøsæter, H., Hoover, C., Hop, H., Hussey, N. E., Nahrgang, J., Steiner, N., Bender, M., Berge, J., Castellani, G., Chernova, N., Copeman, L., David, C. L., Deary, A., Divoky, G., Dolgov, A. V., ... Walkusz, W. (2023). The circumpolar impacts of climate change and anthropogenic stressors on Arctic cod (*Boreogadus saida*) and its ecosystem. *Elementa: Science of the Anthropocene*, 11(1), 00097. <https://doi.org/10.1525/elementa.2022.00097>

Geoffroy, M., Majewski, A., LeBlanc, M., Gauthier, S., Walkusz, W., Reist, J. D., & Fortier, L. (2016). Vertical segregation of age-0 and age-1+ polar cod (*Boreogadus saida*) over the annual cycle in the Canadian Beaufort Sea. *Polar Biology*, 39(6), 1023–1037. <https://doi.org/10.1007/s00300-015-1811-z>

Gorsky, G., Ohman, M. D., Picheral, M., Gasparini, S., Stemmann, L., Romagnan, J. B., Cawood, A., Pesant, S., García-Comas, C., & Prejger, P. (2010). Digital zooplankton image analysis using the Zooscan integrated system. *Journal of Plankton Research*, 32, 285–303. <https://doi.org/10.1093/plankt/fbp124>

Gradinger, R. R., & Bluhm, B. A. (2004). In-situ observations on the distribution and behavior of amphipods and Arctic cod (*Boreogadus saida*) under the sea ice of the high Arctic Canada Basin. *Polar Biology*, 27, 595–603.

Graeve, M., Albers, C., & Kattner, G. (2005). Assimilation and biosynthesis of lipids in Arctic *Calanus* species based on feeding experiments with a ¹³C labelled diatom. *Journal of Experimental Marine Biology and Ecology*, 317, 109–125.

Grainger, E. H., Mohammed, A. A., & Lovrity, J. E. (1986). Copepods in Arctic Sea Ice. *Syllogeus*, 58, 303–310.

Gray, B. P., Norcross, B. L., Blanchard, A. L., Beaudreau, A. H., & Seitz, A. C. (2016). Variability in the summer diets of juvenile polar cod (*Boreogadus saida*) in the northeastern Chukchi and western Beaufort seas. *Polar Biology*, 39, 1069–1080.

Greenacre, M. (2017). 'Size' and 'shape' in the measurement of multivariate proximity. *Methods in Ecology and Evolution*, 8(11), 1415–1424. <https://doi.org/10.1111/2041-210X.12776>

Grömping, U. (2006). Relative importance for linear regression in R: The package relaimpo. *Journal of Statistical Software*, 17(1), 1–27.

Guarino, M., Sime, L., Schröeder, D., Malmierca-Vallet, I., Rosenblum, E., Ringer, M., Ridley, J., et al. (2020). Sea-ice-free Arctic during the last

interglacial supports fast future loss. *Nature Climate Change*, 10(10), 928–932. <https://doi.org/10.1038/s41558-020-0865-2>

Gulliksen, B., & Lønne, O. J. (1989). Distribution, abundance, and ecological importance of marine sympagic fauna in the Arctic. *Rapports et Procès-Verbaux Des Réunions*, 188, 133–138.

Hacunda, J. S. (1981). Trophic relationships among demersal fishes in a coastal area of the Gulf of Maine. *Fisheries Bulletin*, 79, 775–788.

Hop, H., & Graham, M. (1995). Respiration of juvenile Arctic cod (*Boreogadus saida*): Effects of acclimation, temperature, and food intake. *Polar Biology*, 15, 359–367.

Hop, H., & Tonn, W. M. (1998). Gastric evacuation rates and daily rations of Arctic cod (*Boreogadus saida*) at low temperatures. *Polar Biology*, 19, 293–301. <https://doi.org/10.1007/s003000050249>

Hop, H., Tonn, W. M., & Welch, H. E. (1997). Bioenergetics of Arctic cod (*Boreogadus saida*) at low temperatures. *Canadian Journal of Fisheries and Aquatic Sciences*, 54, 1772–1784.

Hopcroft, R. R., & Kosobokova, K. N. (2010). Distribution and egg production of *Pseudocalanus* species in the Chukchi Sea. *Deep-Sea Research II*, 57, 49–56.

Hoppmann, M., Kuznetsov, I., Fang, Y.-C., & Rabe, B. (2022). Mesoscale observations of temperature and salinity in the Arctic Transpolar Drift: a high-resolution dataset from the MOSAiC Distributed Network. *Earth System Science Data*, 14(11), 4901–4921. <https://doi.org/10.5194/essd-14-4901-2022>

Hyslop, E. J. (1980). Stomach contents analysis—A review of methods and their application. *Journal of Fish Biology*, 17, 411–429.

Ivlev, V. S. (1961). *Experimental ecology of the feeding of fishes*. Yale University Press.

Jacobs, J. (1974). Quantitative measurement of food selection. *Oecologia*, 14, 413–417.

Jaspers, C., Hopcroft, R. R., Kiørboe, T., Lombard, F., López-Urrutia, Á., Everett, J. D., & Richardson, A. J. (2023). Gelatinous larvacean zooplankton can enhance trophic transfer and carbon sequestration. *Trends in Ecology and Evolution*, 38(10), 980–993. <https://doi.org/10.1016/j.tree.2023.05.005>

Kattner, G., Hirsche, H. J., & Krause, M. (1989). Spatial variability in lipid composition of calanoid copepods from Fram Strait, the Arctic. *Marine Biology*, 102, 473–480.

Kim, Y.-H., Min, S.-K., Gillett, N. P., Notz, D., & Malinina, E. (2023). Observationally-constrained projections of an ice-free Arctic even under a low emission scenario. *Nature Communications*, 14(1). <https://doi.org/10.1038/s41467-023-38511-8>

Kirkæter, P. (1978). *Biomasseundersøkelse av Calanus finmarchicus i Korsfjorden 1974–1975, belyst ved kalorimetri og biokjemiske analyser*. Unpublished Cand. real. thesis. University of Bergen.

Kohlbach, D., Graeve, M. A., Lange, B., David, C., Peeken, I., & Flores, H. (2016). The importance of ice algae-produced carbon in the central Arctic Ocean ecosystem: Food web relationships revealed by lipid and stable isotope analyses. *Limnology and Oceanography*, 61(6), 2027–2044.

Kohlbach, D., Schaafsma, F. L., Graeve, M., Lebreton, B., Lange, B. A., David, C., Vortkamp, M., & Flores, H. (2017). Strong linkage of polar cod (*Boreogadus saida*) to sea ice algae-produced carbon: Evidence from stomach content, fatty acid and stable isotope analyses. *Progress in Oceanography*, 152, 62–74.

Køie, M. (2009). *Boreogadus saida* (Lepechin)(Gadidae): A review of its metazoan parasite fauna from Greenland, eastern Canada, Alaska and the Russian Arctic. *Polar Biology*, 32, 1399–1406.

Kraft, A., Graeve, M., Janssen, D., Greenacre, M., & Falk-Petersen, S. (2015). Arctic pelagic amphipods: Lipids dynamics and life strategy. *Journal of Plankton Research*, 37(4), 790–809. <https://doi.org/10.1093/plankt/fbv052>

Krumpen, T., von Albedyll, L., Goessling, H. F., Hendricks, S., Juhls, B., Spreen, G., Willmes, S., Belter, H. J., Dethloff, K., Haas, C., Kaleschke, L., Katlein, C., Tian-Kunze, X., Ricker, R., Rostosky, P., Rückert, J., Singha, S., & Sokolova, J. (2021). MOSAiC drift expedition from October 2019 to July 2020: Sea ice conditions from space and comparison with previous years. *The Cryosphere*, 15, 3897–3920. <https://doi.org/10.5194/tc-15-3897-2021>

Kunz, K. L., Frickenhaus, S., Hardenberg, S., Johansen, T., Leo, E., Pörtner, H.-O., Schmidt, M., Windisch, H. S., Knust, R., & Mark, F. C. (2016). New encounters in Arctic waters: a comparison of metabolism and performance of polar cod (*Boreogadus saida*) and Atlantic cod (*Gadus morhua*) under ocean acidification and warming. *Polar Biology*, 39(6), 1137–1153. <https://doi.org/10.1007/s00300-016-1932-z>

Kvile, K. Ø., Ashjian, C., Feng, Z., Zhang, J., & Ji, R. (2018). Pushing the limit: Resilience of an Arctic copepod to environmental fluctuations. *Global Change Biology*, 24, 5426–5439.

Lechowitz, M. J. (1982). The sampling characteristics of electivity indices. *Oecologia*, 52, 22–30.

Liao, H., Pierce, C. L., & Larscheid, J. G. (2001). Empirical assessment of indices of prey importance in the diets of predacious fish. *Transactions of the American Fisheries Society*, 130, 583–591.

Lønne, O. J., & Gulliksen, B. (1989). Size, age and diet of polar cod, *Boreogadus saida* (Lepechin 1773), in ice covered waters. *Polar Biology*, 9, 187–191.

Lønne, O. J., & Gulliksen, B. (1991). On the distribution of sympagic macro-fauna in the seasonally ice covered Barents Sea. *Polar Biology*, 11, 457–469.

Madsen, S. D., Nielsen, T. G., & Hansen, B. W. (2001). Annual population development and production by *Calanus finmarchicus*, *C. glacialis* and *C. hyperboreus* in Disko Bay, western Greenland. *Marine Biology*, 139, 75–83.

Maes, S. M., Christiansen, H., Mark, F. M., Lucassen, M., Van de Putte, A., Volckaert, F. A. M., & Flores, H. (2021). High gene flow in polar cod (*Boreogadus saida*) from West-Svalbard and the Eurasian Basin. *Journal of Fish Biology*, 99, 49–60. <https://doi.org/10.1111/jfb.14697>

Maes, S. M., Schaafsma, F. L., Christiansen, H., Hellemans, B., Lucassen, M., Mark, F. C., Flores, H., & Volckaert, F. A. M. (2022). Comparative visual and DNA-based diet assessment extends the prey spectrum of polar cod *Boreogadus saida*. *Marine Ecology Progress Series*, 698, 139–154. <https://doi.org/10.3354/meps14145>

Majewski, A. R., Walkusz, W., Lynn, B. R., Atchison, S., Eert, J., & Reist, J. D. (2016). Distribution and diet of demersal Arctic cod, *Boreogadus saida*, in relation to habitat characteristics in the Canadian Beaufort Sea. *Polar Biology*, 39, 1087–1098.

Matley, J. K., Crawford, R. E., & Dick, T. A. (2012). Summer foraging behaviour of shallow-diving seabirds and distribution of their prey, Arctic cod (*Boreogadus saida*), in the Canadian Arctic. *Polar Research*, 31(1), 15894. <https://doi.org/10.3402/polar.v31i0.15894>

Matley, J. K., Fisk, A. T., & Dick, T. A. (2013). The foraging ecology of Arctic cod (*Boreogadus saida*) during open water (July–August) in Allen Bay, Arctic Canada. *Marine Biology*, 160, 2993–3004.

McNicholl, D. G., Walkusz, W., Davoren, G. K., Majewski, A. R., & Reist, J. D. (2016). Dietary characteristics of co-occurring polar cod (*Boreogadus saida*) and capelin (*Mallotus villosus*) in the Canadian Arctic, Darnley Bay. *Polar Biology*, 39, 1099–1108. <https://doi.org/10.1007/s00300-015-1834-5>

Melnikov, I. A., & Chernova, N. V. (2013). Characteristics of under-ice swarming of polar cod *Boreogadus saida* (Gadidae) in the central Arctic Ocean. *Journal of Ichthyology*, 53(1), 7–15.

Melnikov, I. A., Kulikov, A. S. 1980. The cryopelagic fauna of the central Arctic Basin. *Biol. Tsentral'nogo Arkticheskogo Basseina*: 97–111 (Canadian translation of *fisheries and aquatic sciences* 4910).

Møller, E. F., & Nielsen, T. G. (2020). Borealization of Arctic zooplankton—Smaller and less fat zooplankton species in Disko Bay, Western Greenland. *Limnology and Oceanography*, 65(6), 1175–1188. <https://doi.org/10.1002/lno.11380>

Nakano, T., Matsuno, K., Nishizawa, B., Iwahara, Y., Mitani, Y., Yamamoto, J., Sakurai, Y., & Watanuki, Y. (2016). Diets and body

condition of polar cod (*Boreogadus saida*) in the northern Bering Sea and Chukchi Sea. *Polar Biology*, 39, 1081–1086.

Nixdorf, U., et al. (2021). MOSAiC extended acknowledgement. Zenodo. <https://doi.org/10.5281/zenodo.5179738>

Norrbin, F., & Bärmstedt, U. (1984). Energy contents in benthic and planktonic invertebrates of Kosterfjorden, Sweden. A comparison of energetic strategies in marine organism groups. *Ophelia*, 23(1), 47–64.

Nowicki, R. C., Borgå, K., Gabrielsen, G. W., & Varpe, Ø. (2023). Energy content of krill and amphipods in the Barents Sea from summer to winter: Variation across species and size. *Polar Biology*, 46, 139–150. <https://doi.org/10.1007/s00300-023-03112-0>

Oksanen, J., Blanchet, F. G., Friendly, M., Kindt, R., Legendre, P., McGlinn, D., Minchin, P. R., O'Hara, R. B., Simpson, G. L., Solymos, P., Stevens, M. H. H., Szoecs, E., & Wagner, H. (2020). *_vegan: Community ecology Package_*. R Package Version, 2, 5–7. <https://CRAN.R-project.org/package=vegan>

Percy, J. A., & Fife, F. J. (1981). The biochemical composition and energy content of Arctic marine macrozooplankton. *Arctic*, 34(4), 307–313.

Pinkas, L., Oliphant, M. S., & Iverson, I. L. K. (1971). Food habits of albacore, bluefin tuna and bonito in Californian waters. *Fish Bulletin*, 152, 1–105.

Polyakov, I. V., Alkire, M. B., Bluhm, B. A., Brown, K. A., Carmack, E. C., Chierici, M., Danielson, S. L., Ellingsen, I., Ershova, E. A., Gårdfeldt, K., Ingvaldsen, R. B., Pnyushkov, A. V., Slagstad, D., & Wassmann, P. (2020). Borealization of the Arctic Ocean in response to anomalous advection from sub-Arctic seas. *Frontiers in Marine Science*, 7, 491, 1–32. <https://doi.org/10.3389/fmars.2020.00491>

R Core Team. (2022). *R: A language and environment for statistical computing*. R Foundation for Statistical Computing. <https://www.R-project.org/>

Rabe, B., Heuzé, C., Regnery, J., Aksenov, Y., Allerholt, J., Athanase, M., Bai, Y., Basque, C., Bauch, D., Baumann, T. M., Chen, D., Cole, S. T., Craw, L., Davies, A., Damm, E., Dethloff, K., Divine, D. V., Doglioni, F., Ebert, F., ... Zhu, J. (2022). Overview of the MOSAiC expedition: Physical oceanography. *Elementa: Science of the Anthropocene*, 10(1), 1–31. <https://doi.org/10.1525/elementa.2021.00062>

Railsback, S. F., & Rose, K. A. (1999). Bioenergetics modeling of stream trout growth: Temperature and food consumption effects. *Transactions of the American Fisheries Society*, 128, 241–256.

Renaud, P. E., Berge, J., Varpe, Ø., Lønne, O. J., Nahrgang, J., Ottesen, C., & Hallanger, I. (2012). Is the poleward expansion by Atlantic cod and haddock threatening native polar cod, *Boreogadus saida*? *Polar Biology*, 35, 401–412. <https://doi.org/10.1007/s00300-011-1085-z>

Roy, D., Haffner, G. D., & Brandt, S. B. (2004). Estimating fish production potentials using a temporally explicit model. *Ecological Modelling*, 173(2–3), 241–257. <https://doi.org/10.1016/j.ecolmodel.2003.09.003>

Runge, J. A., & Ingram, R. G. (1988). Underice grazing by planktonic, calanoid copepods in relation to a bloom of ice microalgae in southeastern Hudson Bay. *Limnology and Oceanography*, 33(2), 280–286.

Schaafsma, F. L., Cherel, Y., Flores, H., Van Franeker, J. A., Lea, M. A., Raymond, B., & Van de Putte, A. P. (2018). Review: The energetic value of zooplankton and nekton of the Southern Ocean. *Marine Biology*, 165, 129. <https://doi.org/10.1007/s00227-018-3386-z>

Schaafsma, F. L., David, C. L., Kohlbach, D., Ehrlich, J., Castellani, G., Lange, B. A., Vortkamp, M., Meijboom, A., Fortuna-Wünsch, A., Immerz, A., Cantzler, H., Klasmeier, A., Zakhrova, N., Schmidt, K., Van de Putte, A. P., Van Franeker, J. A., & Flores, H. (2022). Allometric relationships of ecologically important Antarctic and Arctic zooplankton and fish species. *Polar Biology*, 45, 203–224. <https://doi.org/10.1007/s00300-021-02984-4>

Schmidt, K., Atkinson, A., Petzke, K. J., Voss, M., & Pond, D. W. (2006). Protozoans as a food source for Antarctic krill, *Euphausia superba*: Complementary insights from stomach content, fatty acids and stable isotopes. *Limnology and Oceanography*, 51(5), 2409–2427.

Schulz, K., Koenig, Z., & Muilwijk, M. (2023). The Eurasian Arctic Ocean along the MOSAiC drift (2019–2020): Core hydrographic parameters. Arctic Data Center. <https://doi.org/10.18739/A21J9790B>

Schulz, K., Mohrholz, V., Fer, I., Janout, M. A., Hoppmann, M., Schaffer, J., Koenig, Z., Rabe, B., Heuzé, C., Regnery, J., Allerholt, J., Fang, Y.-C., He, H., Kanzow, T., Karam, S., Kuznetsov, I., Kong, B., Liu, H., Muilwijk, M., ... Tippenhauer, S. (2022). Turbulent microstructure profile (MSS) measurements from the MOSAiC drift, Arctic Ocean [Data set]. PANGAEA. <https://doi.org/10.1594/PANGAEA.939816>

Scott, C. L., Kwasniewski, S., Falk-Petersen, S., & Sargent, J. R. (2000). Lipids and life strategies of *Calanus finmarchicus*, *Calanus glacialis* and *Calanus hyperboreus* in late autumn, Kongsfjorden, Svalbard. *Polar Biology*, 23, 510–516.

Sikora, W. B., Heard, R. W., & Dahlberg, M. D. (1972). The occurrence and food habits of two species of hake *Urophycis regius* and *Urophycis floridanus* in Georgia estuaries. *Transactions of the American Fisheries Society*, 101, 513–516.

Snoeijs-Leijonmalm, P., Flores, H., Sakinan, S., Hildebrandt, N., Svenson, A., Castellani, G., Vane, K., Mark, F. C., Heuzé, C., Tippenhauer, S., Niehoff, B., Hjelm, J., Hentati Sundberg, J., Schaafsma, F. L., Engelmann, R., & the EFICA-MOSAiC Team. (2022). Unexpected fish and squid in the central Arctic deep scattering layer. *Science Advances*, 8(7), 1–17. <https://doi.org/10.1126/sciadv.abj7536>

Snoeijs-Leijonmalm, P., Flores, H., Volkaert, F., Niehoff, B., Schaafsma, F. L., Hjelm, J., Hentati-Sundberg, J., Niiranen, S., Crépin, A. S., Österblom, H. (2020). Review of the research knowledge and gaps on fish populations, fisheries and linked ecosystems in the Central Arctic Ocean (CAO). European Commission Publications Office. <https://op.europa.eu/en/publication-detail/-/publication/aae1e59e-46fe-11ea-b81b-01aa75ed71a1/language-en>

Snoeijs-Leijonmalm, P., Gjøsæter, H., Ingvaldsen, R. B., Knutsen, T., Korneliussen, R., Ona, E., Skjoldal, H. R., Stranne, C., Mayer, L., & Jakobsson, M. (2021). A deep scattering layer under the north pole pack ice. *Progress in Oceanography*, 194, 102560. <https://doi.org/10.1016/j.pocean.2021.102560>

Sutela, T., & Huusko, A. (2000). Varying resistance of zooplankton prey to digestion: Implications for quantifying larval fish diets. *Transactions of the American Fisheries Society*, 129, 545–551.

Swalethorpe, R., Kjellerup, S., Dünweber, M., Nielsen, T. G., Møller, E. F., Rysgaard, S., & Hansen, B. W. (2011). Grazing, egg production, and biochemical evidence of differences in the life strategies of *Calanus finmarchicus*, *C. glacialis* and *C. hyperboreus* in Disko Bay, western Greenland. *Marine Ecology Progress Series*, 429, 125–144.

Thanasssekos, S., & Fortier, L. (2012). An individual based model of Arctic cod (*Boreogadus saida*) early life in Arctic polynyas: I. Simulated growth in relation to hatch date in the northeast water (Greenland Sea) and the north water (Baffin Bay). *Journal of Marine Systems*, 93, 25–38. <https://doi.org/10.1016/j.jmarsys.2011.08.003>

Tippenhauer, S., Vredenborg, M., Heuzé, C., Ulfsbo, A., Rabe, B., Granskog, M. A., Allerholt, J., Balmonte, J. P., Campbell, R. G., Castellani, G., Chamberlain, E., Creamean, J., D'Angelo, A., Dietrich, U., Drost, E. S., Eggers, L., Fang, Y.-C., Fong, A. A., Gardner, J., ... Zhuang, Y. (2023a). Physical oceanography based on Ocean City CTD during POLARSTERN cruise PS122 [Data set]. PANGAEA. <https://doi.org/10.1594/PANGAEA.959964>

Tippenhauer, S., Vredenborg, M., Heuzé, C., Ulfsbo, A., Rabe, B., Granskog, M. A., Allerholt, J., Balmonte, J. P., Campbell, R. G., Castellani, G., Chamberlain, E., Creamean, J., D'Angelo, A., Dietrich, U., Drost, E. S., Eggers, L., Fang, Y.-C., Fong, A. A., Gardner, J., ... Zhuang, Y. (2023b). Physical oceanography based on ship CTD during POLARSTERN cruise PS122 [Data set]. PANGAEA. <https://doi.org/10.1594/PANGAEA.959963>

Tittensor, D. P., Novaglio, C., Harrison, C. S., Heneghan, R. F., Barrier, N., Bianchi, D., Bopp, L., Bryndum-Buchholz, A., Britten, G. L., Büchner, M., Cheung, W. W. L., Christensen, V., Coll, M., Dunne, J. P.,

Eddy, T. D., Everett, J. D., Fernandes-Salvador, J. A., Fulton, E. A., Galbraith, E. D., ... Blavhard, J. L. (2021). Next-generation ensemble projections reveal higher climate risks for marine ecosystems. *Nature Climate Change*, 11, 973–981. <https://doi.org/10.1038/s41558-021-01173-9>

Van Franeker, J. A., Flores, H., & Van Dorssen, M. (2009). The surface and under ice trawl (SUIT). In H. Flores (Ed.), *Frozen desert alive. Dissertation* (pp. 181–188). University of Groningen.

Vane, K., Cobain, M. R. D., Trueman, C. N., Vonnahme, T. R., Rokitta, S., Polunin, N. V. C., & Flores, H. (2023). Tracing basal resource use across sea-ice, pelagic, and benthic habitats in the early Arctic spring food web with essential amino acid carbon isotopes. *Limnology and Oceanography*, 68, 862–877. <https://doi.org/10.1002/limo.12315>

Walkusz, W., Majewski, A., & Reist, J. D. (2013). Distribution and diet of the bottom dwelling Arctic cod in the Canadian Beaufort Sea. *Journal of Marine Systems*, 127, 65–75.

Werner, I., & Gradinger, R. (2002). Under-ice amphipods in the Greenland Sea and Fram Strait (Arctic): Environmental controls and seasonal patterns below the pack ice. *Marine Biology*, 140, 317–326.

Werner, I., & Martinez-Arribalzaga, P. (1999). The sub-ice fauna of the Laptev Sea and the adjacent Arctic Ocean in summer 1995. *Polar Biology*, 21, 71–79.

Wickham, H. (2015). *ggplot2: Elegant graphics for data analysis*. Springer-Verlag.

Wollenburg, J. E., Iversen, M., Katilein, C., Krumpen, T., Nicolaus, M., Castellani, G., Peeken, I., & Flores, H. (2020). New observations of the distribution, morphology and dissolution dynamics of cryogenic gypsum in the Arctic Ocean. *The Cryosphere*, 14, 1795–1808. <https://doi.org/10.5194/tc-14-1795-2020>

SUPPORTING INFORMATION

Additional supporting information can be found online in the Supporting Information section at the end of this article.

How to cite this article: Schaafsma, F. L., Flores, H., David, C. L., Castellani, G., Sakinan, S., Meijboom, A., Niehoff, B., Cornils, A., Hildebrandt, N., Schmidt, K., Snoeijs-Leijonmalm, P., Ehrlich, J., Ashjian, C. J., & the MOSAiC team ECO (2024). Insights into the diet and feeding behavior of immature polar cod (*Boreogadus saida*) from the under-ice habitat of the central Arctic Ocean. *Journal of Fish Biology*, 105(3), 907–930. <https://doi.org/10.1111/jfb.15836>